

**Geology of sediment core retrieved from Caranzalem beach ,  
Tiswadi ,Goa**

A Dissertation Report for

GEO-651: Dissertation

Credits: 16

Submitted in partial fulfillment of Masters Degree

MSc Applied Geology

by

**VEENA VISHWAS NAIK**

22P0450028

128861714883

201909272

Under the Supervision of

**Dr. A. A. A. VIEGAS**

School of Earth, Ocean and Atmospheric Science, Applied Geology



**GOA UNIVERSITY**

**MAY 2024**

Examined by :



Seal of the School

## DECLARATION BY STUDENT

I declare that the information presented in this Dissertation report titled " Geology Of Sediment Core Retrieved From Caranzalem Beach, Tiswadi, Goa" is derived from research conducted by me during my M.Sc. Applied Geology program at the School of Earth, Ocean, and Atmospheric Sciences, Goa University. This research was conducted under the supervision of Dr. A.A.A.A. VIEGAS, Associate Professor, Applied Geology, SEOAS. I affirm that this work has not been submitted elsewhere for the purpose of obtaining a degree or diploma.

Furthermore, I acknowledge that the accuracy of observations, experiments, and other findings presented in the dissertation is my responsibility, and Goa University or its authorities will not be held accountable for any discrepancies.

I grant authorization to the University authorities to upload this dissertation to the dissertation repository or any other platform as per UGC regulations, making it accessible to anyone as required.



Veena Vishwas Naik

Seat No. 22P0450028

02 May 2024

Goa University

COMPLETION CERTIFICATE

This is to certify that the dissertation report Geology of Sediment Core Retrieved From Caranzalem Beach , Tiswadi ,Goa is a bonafide work carried out by Ms. Veena Vishwas Naik under my supervision in partial fulfillment of the requirements for the award of the degree of Master of Science in the Discipline Applied Geology at the School of Earth Ocean And Atmospheric Sciences, Goa University.

  
Dr. A.A.A.A Viegas

Vice Dean( Academics) , SEOAS

Date: 2/3/2024

  
3/1/24

Dean: Dr. Sanjeev C. Ghadi

Senior Professor

School of Earth Ocean and Atmospheric Sciences

May 2024

Goa University



**Geology of sediment core retrieved from Caranzalem beach ,**

**Tiswadi ,Goa**

A Dissertation Report for

GEO-651 Dissertation

Credits: 16

Submitted in partial fulfilment of Master's Degree

MSc in Applied Geology

by

**VEENA VISHWAS NAIK**

22P0450028

128861714883

201909272

Under the Supervision of

**Dr. A. A. A. A. VIEGAS**

School of Earth, Ocean and Atmospheric Sciences

Applied Geology



**GOA UNIVERSITY**

**May 2024**

**Geology of sediment core retrieved from Caranzalem beach ,  
Tiswadi ,Goa**

A Dissertation Report for

GEO-651: Dissertation

Credits: 16

Submitted in partial fulfillment of Masters Degree

MSc Applied Geology

by

**VEENA VISHWAS NAIK**

22P0450028

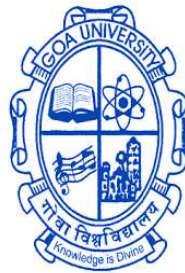
128861714883

201909272

Under the Supervision of

**Dr. A. A. A. A. VIEGAS**

School of Earth, Ocean and Atmospheric Science, Applied Geology



**GOA UNIVERSITY**

**MAY 2024**

Examined by :

Seal of the School

## **DECLARATION BY STUDENT**

I declare that the information presented in this Dissertation report titled “ Geology Of Sediment Core Retrieved From Caranzalem Beach, Tiswadi, Goa" is derived from research conducted by me during my M.Sc. Applied Geology program at the School of Earth, Ocean, and Atmospheric Sciences, Goa University. This research was conducted under the supervision of Dr. A.A.A.A. VIEGAS, Associate Professor, Applied Geology, SEOAS. I affirm that this work has not been submitted elsewhere for the purpose of obtaining a degree or diploma.

Furthermore, I acknowledge that the accuracy of observations, experiments, and other findings presented in the dissertation is my responsibility, and Goa University or its authorities will not be held accountable for any discrepancies.

I grant authorization to the University authorities to upload this dissertation to the dissertation repository or any other platform as per UGC regulations, making it accessible to anyone as required.

Signature and Name of Student

Seat No. 22P0450028

Date :

Place: Goa University

## **COMPLETION CERTIFICATE**

This is to certify that the dissertation report Geology of Sediment Core Retrieved From Caranzalem Beach , Tiswadi ,Goa is a bonafide work carried out by Ms. Veena Vishwas Naik under my supervision in partial fulfillment of the requirements for the award of the degree of Master of Science in the Discipline Applied Geology at the School of Earth Ocean And Atmospheric Sciences, Goa University.

Dr. A.A.A.A Viegas

Date:

Dean: Dr. Sanjeev C. Ghadi

School stamp

Senior Professor

School of Earth Ocean and Atmospheric Sciences

Date:

Place: Goa University

**CONTENT**

SR. NO.	TITLE	PAGE NO.
	ACKNOWLEDGEMENTS	vi
	LIST OF TABLES	vii
	LIST OF FIGURES	viii
1	CHAPTER 1: INTRODUCTION.	
	Prologue	1-2
	Aim and objective	3
2	CHAPTER II: LITERATURE REVIEW	
	Geology of Goa	4-10
	Strucure and Tectonics.	11
	Geomorphology	12-13
	Sea Level Changes	14-16
	Literature Review	17
3	CHAPTER III: METHODOLOGY	
	Geology of the Study Area	18-19
	Grain Size	20-24

	X-ray diffraction	25-28
	Munsell Chart	28-29
	Clay Mineralogy	30-33
	Sample Preparation	34-38
4	CHAPTER IV: OBSERVATION AND DISCUSSION	
	Grain Size Data	39-45
	Clay Mineralogy	46-54
	Lithology of Study Area	55
	Interpretation	56-57
	Result	58
	References	59- 61

## ACKNOWLEDGEMENTS

I would like to begin by expressing my deepest gratitude to my guide, Dr. Anthony A.A.A. Viegas. His invaluable guidance and support throughout every step of this thesis have been instrumental in its completion. His mentorship has been crucial to the completion of this work. Thank you for your unwavering commitment and understanding over the past year.

My sincere thanks also go to Dr. Niyati Kalangutkar, Dr. Poornima Sawant, Dr. Nicole Sequeira, Dr. Pooja Ghadi and Mr. Mahesh Mayekar for their continuous support and encouragement during this journey.

I extend my heartfelt gratitude to Rajdeep Builders for generously providing the samples and data..

I would also like to express my deepest thanks to all the administrative staff and laboratory assistant at the School of Earth, Ocean, and Atmospheric Sciences, Goa University. Your assistance has been instrumental in my research endeavors.

I would like to acknowledge my fellow colleagues Roshni Pujari and Shavari Surlikar for their companionship, stimulating discussion we had.

Special thanks to Divya Fulari, Dixita Vengurlekar, Kaif Jamkhandi, Aaron Pereira and Rhys Saldanha for their steadfast support throughout this process.

Lastly, I would like to express my heartfelt gratitude to my parents for their unconditional love, encouragement, and belief in my abilities. Their support has been the foundation of my academic achievements, and I am forever grateful. Thank you all for your significant contributions and for making this experience a memorable one.

## **LIST OF TABLES**

<b>Table No.</b>	<b>Description</b>	<b>Page No.</b>
Table No:01	Lithostratigraphic Classification Of Supracrustal Rocks From Goa	6
Table No:02	Summary Of The Geomorphological Evolution Of Goa	16
Table No:03	Wentworth Grain Size Scale For Siliclastic Sediment	22
Table No: 04	Methods of measuring sediment grain size	23
Table No:05	Grain Size Data	39
Table No:06	Descriptive Terminology Of The 3 Component Sand-Silt-Clay Sedimentary System	41
Table No:07	Graphical Grain Size Parameters For Sediment Samples	44
Table No:08	Identification Of Clay Mineral	54

## **LIST OF FIGURES**

<b>Table No.</b>	<b>Description</b>	<b>Page No.</b>
Figure No:1	Geological Map Of Goa	4
Figure No:2	Location Map Of Study Area	19
Figure No: 3	Samples Kept For Soaking	35
Figure No: 4	Samples sterilised from organisms	35
Figure No:5	Samples kept for settling in 1000 ml volumetric cylinder	36
Figure No:6	10 ml pipetted out for XRD	36
Figure No: 7	Samples kept for drying in oven	37
Figure No: 8 & 9	XRD Rigaku machine	38
Figure No: 10	Diagram showing sand-silt-clay texture	39
Figure No: 11	Ternary diagram for sand-silt-clay mixture	40
Figure No: 12	Ternary diagram for hydrodynamic condition	40
Figure No:13	Ternary diagram for classification of hydrodynamic condition	45
Figure No: 14	Lithology Of Study Area	55
Graph No.1-3	Grain Size Analysis	42-43
Graph No. 4- 15	XRD Analysis Of Clay Minerals	46- 53

# **CHAPTER I – INTRODUCTION**

## PROLOGUE

Goa, a diminutive emerald region situated along the western coast of India, is a coastal state celebrated for its exquisite beaches, picturesque landscapes, and culturally rich heritage. Characterized by diverse geological formations, this state provides insights into its geological history. Positioned between latitudes  $14^{\circ}53'54''$  N and  $15^{\circ}40'00''$  N and longitudes  $73^{\circ}40'33''$  E and  $74^{\circ}20'13''$  E, Goa spans an area of 3,702 square kilometers, encompassing two revenue districts: North Goa and South Goa. Its boundaries are defined by the Terekhol River in the north, demarcating it from Maharashtra, and in the east and south by Karnataka State, with the Arabian Sea to the west. Goa resides on the Western Coast of India, and has a 104 km long coastline.

Topographically intricate from west to east, Goa can be categorized into three primary physiographic units: a spacious coastal plain, an undulating midland hilly region, and the Western Ghats. The distance between the Ghats and the sea is about 40 km, with scattered hills throughout the strip. The coastal-estuarine plains consist of linear beaches, complemented by sand dunes, wetlands, rivers, and intersected rocky promontories. The midlands feature mountainous, lateritized plateau-capped hills, predominantly covered with lush vegetation. Further inland lie the towering peaks of the forested Western Ghats.

Geologically, Goa is positioned in the northwestern part of the Western Dharwar Craton, where the Shimoga-Goa supracrustal belt extends continuously beneath the Arabian Sea and the Deccan Traps to the north. This belt potentially extends beneath the Traps up to the Narmada, where the Narmada-Son lineament terminates this supracrustal belt. The Shimoga-Goa belt spans NNW-SSE over a length of approximately 250 km, with a maximum width of about 120 km at Dharwar.

The western boundary of the Shimoga-Goa supracrustal belt is delineated by extensive domal masses of gneissose rocks, exemplified by formations like the Chandranath granite gneiss and the Canacona granite. In contrast, the eastern margin is marked by faulting, while the southern region indicates deposition in shallow waters. The northern section of the basin is dominated by a substantial sequence of greywackes. Conversely, the southern section is characterized by an association of orthoquartzite and basic lava, indicative of subaerial environments and intermittent volcanic activity within a coastal sand setting under stable conditions.

The limestone-iron-manganese ore sequence found in Goa and north Kanara (Castlerock band) in the northern part of the Shimoga belt, maintains physical continuity with its counterpart in the southern part. This sequence serves as a marker horizon, illustrating the consistent nature of rocks across the entire length of the belt. The granitic-gneisses originating from Goa have been ascribed either syntectonic or post-tectonic status in relation to the deformations observed in the supracrustals. However, a notable lack of clarity exists regarding the interrelationships among the granitic gneisses and between the gneisses and the supracrustal greenstones. The supracrustal sequences, comprising metavolcanics and clastics, each exhibit distinct characteristics, yet both are classified under the stratigraphic group known as the Goa Group, (Gokul et al., 1985). Situated well within the tropics and flanked by the Arabian Sea to the west and the Western Ghats to the east, the area has a tropical maritime and monsoon type of climate. Other climatic features include regular monsoon rains i.e, the summer monsoon from SW winds.

## **AIM AND OBJECTIVE**

The aim of this study was to analyze borehole retrieved data from Caranzalem beach estuarine sediments, focusing on sedimentary characteristics, sediment mineralogy (including clay minerals).

To Conduct megascopic analysis to identify the lithology of remnants of country rock encountered at the base of the sediment core.

- Perform XRD analysis on samples from different depths to identify the various minerals present.
- Characterize sediment to delineate the sediment fractions across various depths.
- Plot these fractions on a Perjup diagram to understand hydrodynamic conditions.
- Index colors present in the sediment core according to the Munsell color chart.
- Combine all collected data to create a comprehensive log.

# **CHAPTER II – LITERATURE REVIEW**

## GEOLOGY OF GOA

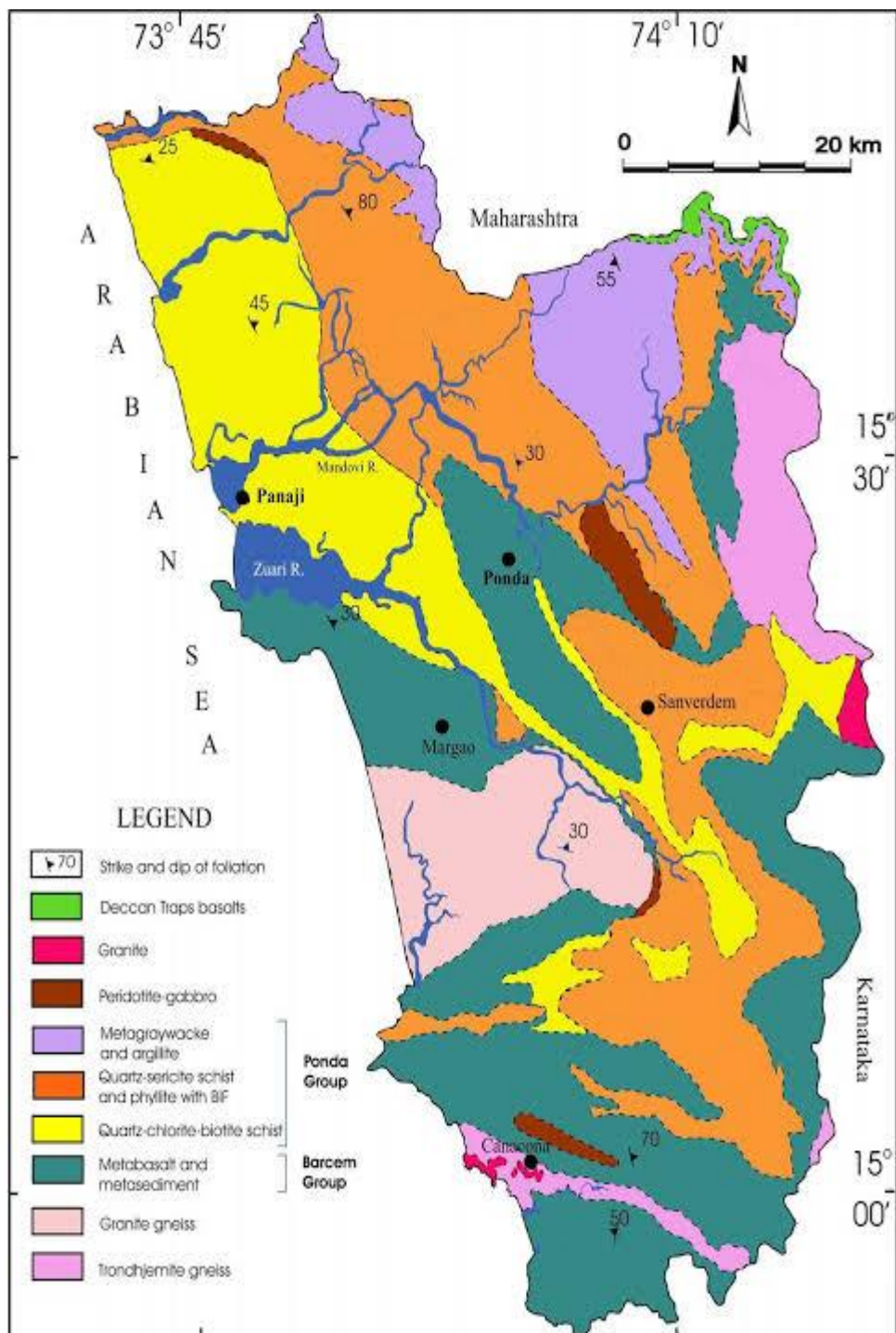


Figure No: 1: Geological sketch map of Goa (after Dessai,2018)

The supracrustal assemblages constituting the Goa Group, ( Gokul et al.,1985), can be delineated into two distinct lithostratigraphic sequences: the Barcem Group and the Ponda Group, (Dessai , 2011). The former is predominantly composed of greenstones (metabasalts) and overlies a basement comprising the 3400-3300 Ma Anmode Ghat trochjemitic gneiss, featuring a crudely developed quartz-pebble conglomerate at its base. The Barcem Group exhibits lithological affinities with the lower section of the Bababudan Group.

The latter, identified as the Ponda Group, constitutes a younger lithostratigraphic sequence primarily dominated by clastic formations. This group is formally equivalent to the Chitradurga Group within the Dharwar Super Group. It rests upon a basement composed of the 2900-2700 Ma Chandranath granite gneiss, marked by a distinctive unconformity characterized by a polymict, granite-clast metaconglomerate. This conglomerate shares notable similarities with the Talya conglomerate found at the base of the Chitradurga Group. Overlying this conglomerate is a psammitic sequence, succeeded by chemogenic sediments hosting the Banded Iron Formation (BIF) and a deep-water turbidite sequence (argillite-graywacke association) with intercalations of mafic volcanics. The supracrustal sequence is intruded by the Bondla layered mafic-ultramafic complex. Within the Ponda Group, three distinct formations are recognized: Sanvordem, Bicholim, and Vagheri. (D.D, Arolkar,1995)

## RESIDUAL ROCKS.

## LATERITES

Basic Intrusives (late)	65-56 Ma	Dolerites
Deccan Traps	67-64 Ma	Basalt
Basic Intrusives		Metadolerites
Bondla Mafic - ultramafic layered complex		Dunite-peridotite-gabbro complex and equivalents
	Vagheri Formation	Metabasalts, Argillites and Metagreywacke
Ponda Group	Bicholim Formation	Banded ferruginous Quartzite, Manganiferous Cherthala vrecchia with pink ferruginous phyllite
	Sanvordem Formation	Metagreywacke, Argillites, Quartzite, Tilloid
	-----Unconformity----- ----	
Barcem Group	Barcem	Metagabbro ,peridotite,talc- chlorite schist,Quartzite, Quartz-sericite-schist,Red phyllite,Quartz porphyry Massive,Schistose and vesicular metabasalt
	-----Unconformity----- ---	
Canacona Granite	2979 + 4 Ma	Porphyritic potassic granite
Chandranath Granite Gneiss	2900-2700 Ma	Granodiorite
Anmode Ghat Trondhjemite gneiss	3400-3300 Ma	Basement; Trondhjemite - tonality- granodiorite

Table No.1:Revised lithostratigraphic classification of supracrustal rocks from Goa (Dessai , 2011)

### **Barcem Group**

The Barcem Group, positioned as the older lithostratigraphic unit, is formally identified resting on a basement comprised of 3400-3300 Ma Anmode Ghat trondhjemite gneiss. Within this group, meta-volcanic and meta-sedimentary formations are discernible. The meta-volcanics encompass basic and acidic lavas, agglomerates, and tuffs, while the metasediments comprise quartzites, quartz-sericite-schists, quartz-chlorite-schists, and minor phyllites. Notably, the Barcem Group is unconformably overlain by the Ponda Group.

### **Ponda Group**

The Ponda Group, prominently manifested around Ponda town with well-exposed lithologies, comprises three formations in ascending order: Sanvordem Formation, Bicholim Formation, and Vagheri Formation. These formations are predominantly characterized by clastic sediments, with mafics being subordinate, primarily in the Vagheri Formation. The total thickness of the Ponda Group around Ponda is approximately 8.8 km.

### **Sanvordem Formation**

The Sanvordem Formation, the basal unit of the Ponda Group, rests on the Chandranath granite gneiss and is marked by a polymict metaconglomerate at its base. Comprising metagreywacke and argillites, the conglomerate exhibits stretched and elongated pebbles in a schistose chlorite matrix. Lithological variations are notable, and exposures along the railway track between Sanvordem railway station and Periudoc reveal a thickness exceeding 1.2 km. The formation displays features such as metagreywacke, metaconglomerate intercalations, and thinly bedded

resembling calcareous mudstones or siltstones, contain calcite, dolomite, ankerite, siderite, and tremolite.

### **Vagheri Formation**

The uppermost stratum of the Ponda Group, known as the Vagheri Formation, conformably overlies the Bicholim Formation and exhibits optimal exposure northeast of Valpoi. This formation is predominantly composed of metagreywackes with subordinate metabasalts. The coarse-grained metagreywackes, displaying a grey to grayish-green hue, are compact and exhibit poorly developed schistosity. Notably, there is evident alteration between fine sediments (shales, mudstones, siltstones or argillites) and coarse sediments (greywackes).

The metagreywackes showcase graded bedding, with the fine-grained greywackes (sandstones) exhibiting lamination, current ripples, and convolute lamination. Minimal compositional variation is observed both laterally and vertically, except for alterations in sandstones and shales. The base surfaces of sandstones frequently exhibit sole markings. Comprising angular to subangular crystic and lithic fragments of limestones and phyllites (derived from the Bicholim Formation), the sandstones feature a fine clay-size matrix composed of quartz, feldspar, and chlorite.

Metabasalts within the Vagheri Formation appear as narrow, lenticular intercalations resembling sill-like bodies within the metagreywacke. These metabasalts, grey to greenish-grey, are hard, compact, and exhibit faint schistosity. Mineralogically, they consist of chlorite, tremolite/actinolite (pseudomorphous after clinopyroxene), plagioclase (saussuritized), epidote, zoisite, opaques, and secondary quartz.

argillites. The metaconglomerate consists of stretched lenticular pebbles and boulders enclosed in a schistose matrix dominated by chlorite. The metagreywackes, metamorphosed sandstones, exhibit graded bedding and consist of sub-angular quartz, plagioclase, lithic fragments, and matrix of sericite, chlorite, and quartz. Argillites are light to deep grey and comprise quartz in a sericite-chlorite matrix with opaques.

The Sanvordem Formation is characterized by a stratigraphic sequence of thin-bedded argillites, displaying divisions corresponding to the Bouma's turbidite sequence (1962). The presence of sandstone dykes and sills, slump folds within megabeds, and variations in form indicate a complex geological history. Gravity flow turbidites are recognized, categorized as low-density flows, and could be interpreted as distal turbidites based on sedimentary structures and typical sequences observed. The lower and upper parts of the Sanvordem Formation might represent proximal and distal turbidite deposits, respectively. (G,Fernandes.et.al, 2022)

### **Bicholim Formation**

The Bicholim Formation, situated above the Sanvordem Formation, extends across the entire length of Goa (-185km) in a NW-SE direction from Naibag (2 km NE of Pernem) in the north to Salgini in the south, with an average true thickness of about 1,400 m (Gokul, 1985). Comprising ferruginous and manganiferrous phyllites, banded ferruginous quartzites, quartz-chlorite-amphibole schists, and minor impure limestones (referred to as calcareous phyllite at times), this formation hosts a substantial horizon of banded iron formation (BIF) nestled between the ferruginous phyllites.

The BIF includes banded haematite quartzites (BHQ) and banded magnetite quartzites (BMQ), occurring as intercalations within the phyllites. The phyllites reciprocally intercalate within the BHQs/BMQs, forming a dynamic relationship dependent on their relative proportions at a given location. BHQs are sometimes intercalated by pyritiferous-carbonaceous shales and talcose chlorite-schists. The BHQs, rich in iron, serve as protores for iron ore deposits confined to this formation. Towards the south, BHQs become thinner and less rich in iron, appearing as impersistent bands and lenses within the phyllites. Protores to the northwest contain a higher percentage of haematite, while those to the south, especially between Darguem and Viliena, contain magnetite. Southward, manganese-rich lenses within the phyllites become more prevalent, especially between Sanguem and Salgini.

Mafic dykes, termed 'edidiorites,' traverse the BHQs and are completely altered to clay minerals. BHQs exhibit various primary sedimentary structures, including bedding, meso- and micro-bands of iron oxide and silica, current-dominated ripples, and penecontemporaneous deformation structures such as brecciation, slumps, and faults. Post-depositional structures encompass pinch and swell structures, pods, syneresis cracks, and desiccation features.

The dominant lithology, ferruginous phyllite, comprises quartz, chlorite, and sericite mica, imparting a silky sheen to cleavage surfaces. Amphibole schists include tremolite, chlorite, quartz, and opaques. BHQs are thinly laminated, consisting of alternate laminae of haematite/magnetite, chert, and chamosite (Fe-Chlorite). Maritisation, the replacement of magnetite by haematite, is common. Rare limestones associated with the phyllites exhibit biogenic structures like stromatolites, indicating evidence of microbial life. Some rocks within this category,

## **STRUCTURE AND TECTONICS**

The geological setting of the Goa Group of rocks is characterized by a general NW-SE orientation, experiencing three phases of folding in its history. The initial folding (F1) imparted a WNW-ESE strike to the rocks, particularly evident in the southern part of the state, associated with the Chandranath granite dated at 2650±100 Ma. The second folding stage (F2) resulted in NW-SE striking folds, prominently found in north-central and northeastern Goa, with the Western Ghat granite gneiss being syntectonic. The third folding phase (F3) produced northwesterly plunging broad synclinal folds in the northeastern parts of Goa. (Dessai, et al, 1994)

The straight coastline suggests a major fault along the west coast, associated with weak planes. In South Goa, intense folding is observed with vertical or steeply dipping metamorphic layering (schistosity and gneissosity) exhibiting the same WNW-ESE strike. In north Goa, rocks have a NW-SE strike parallel to the coast, gently dipping and lacking prominent schistosity. The Western Ghat fault, extending from NS to NNW-SSE, is a notable fault zone. Field observations are limited due to intense laterization, with unweathered rocks exposed primarily in coastal headlands or along steep slopes of high hill ranges.

## GEOMORPHOLOGY

Goa's topography comprises rolling hills, beaches, and segments of the Western Ghats, displaying a polycyclic landscape shaped predominantly during the Cenozoic era under humid tropical conditions. The landforms result from the intricate interplay of the Indian plate's eastward movement from Gondwana, followed by epeirogenic uplift and subsidence, influenced by climatic shifts and eustatic sea level variations. The 100km coastline exhibits diverse features, with Salcete, Bardez, and Pernem hosting long sandy stretches, while Canacona-Quepem and Marmagoa display crenulated and indented coasts. Coastal plains and terraces lie below 10m above sea level, low tablelands at 10-100m, intermediate tablelands and denudational hills at 150-300m, and the Western Ghats plateau at 600-700m. Major rivers like Tiracol, Mandovi, Zuari, Sal, Talpona, and Galgibaga flow through Goa, with Mandovi and Zuari being relatively prominent. All rivers are estuarine, allowing tidal penetration several kilometers inland. Zuari originates in the Western Ghats in Karnataka, covering over 70 km before meeting the Arabian Sea at Mormugao, with significant tributaries such as Guloli, Sanguem, and Kushavati.

(Nayak, 2020)

The drainage in Goa is dominated by two directions: directly to the sea (from east to west), and the NW or NNW direction in accordance with the geological structure. The Mandovi widens to approximately 4km at Aguada Bay, with an average depth of about 5m. The Siquerim River merges with the bay, and upstream for 6km, the channel narrows to around 750m wide and 5m deep. The Mhapsa River meets the Mandovi at the upper end of this stretch. Further up, Diwar Island splits the Mandovi into two channels, which reunite after passing through marshy terrain. The

The sediments documented in various locations in Goa, such as Sangod iron ore mine, Dabolim railway station, Goa University Campus, Taleigao, Tivim, and others, including carbonaceous materials and plant remains, likely originated in fluvio-lacustrine or lagoonal environments during a transgressive phase around 2.3-1.5 ka BP. Similar occurrences of clayey and silty sediments are found in bore wells, supported by lithified beach rock around Korlai-Borlai and along the Konkan coast to the north of Goa (Dessai, 2018).

Marine shell beds in intertidal regions of Chapora, Mandovi, Zuari, and other rivers suggest palaeo-sea inlets linked to sea level oscillations between 2.3-1.5 ka BP. These oscillations likely contributed to the formation of tidal flats on the west coast. Features like abrasional platforms, sea stacks, sea caves at Aguada, and beach rocks at Anjuna and Bogmalo, situated above present sea levels, are associated with this past sea level rise. Palaeodunes (stabilized dunes) further indicate higher past sea levels, while the presence of fossil wood in calcareous aeolianite, 6.5 m below the dune surface, suggests a subsequent sea level lowering by 1.5-2.5 m below present-day MSL (Kale, 1983). The combined evidence of beach rock and aeolianite indicates fluctuations in sea level. While the present-day sea level corresponds roughly to conditions around 6.0 ka BP, contemporary local sea level rise, particularly in Goa, may be linked to neotectonic activity or eustatic base level changes (Dessai, 2018).

Cumbarjua canal joins the Mandovi about 4km upstream from Diwar Island. As the main channel progresses 30km from Diwar Island to Ganjem, it becomes narrower and shallower. Along this stretch, rivers Dicholi, Valvat, Kudnem, and Khandepar join the Mandovi, with the latter being the largest and fed by the Dudhsagar River. Near Ganjem, the Mhadei River, along with Ragda River, contribute runoff to the Mandovi during monsoons. The Mhapsa River, joined by the rivers Asnoda and Moide, flows into the Mandovi at Penha de France, accompanied by a network of smaller rivulets passing through marshes .

## **SEA LEVEL CHANGES**

Successive sea level oscillations have given rise to a diverse range of coastal landforms, encompassing both aggradational and degradational features. (Ahmed, 1972) categorizes the Western coast of India, including Goa, as a coast of submergence based on evidence such as sea cliffs, abrasional platforms, rocky promontories, tidal flats, anastomosing drainage, and laterite at depths of 20 to 30 m below mean sea level. Conversely, indications of recent emergence are observed in extensive beaches, offshore rocky islands, sea caves, beach rocks, and littoral terraces (Dessai, 2018).

The coastal morphology exhibits evolutionary features related to the post-Flandrian transgression, with the present sea level established during the mid-Holocene (Bardahn, et.al, 2011). The Goa coast provides ample evidence of sea level changes post-mid Holocene, with late Quaternary periods witnessing a lowering of sea levels, evident in shelf-edge ridges dated to 7.5 and 11.0 ka BP (Nair and Hashimi, 1980; Rao and Nair, 1992), possibly indicating palaeo-shorelines.

During the late Quaternary (Pleistocene-Holocene transition), the sea level was substantially lower, approximately 60-90 m below the present level, as evidenced from raised cliffs, river terraces, sea-level laterites, and estuarine features at depths of 20-34 m below MSL (Feio, 1956). This regression led to deep entrenched river valleys bordered by raised laterite tablelands. Subsea-level laterites near Cansaulim and comparable formations in Dapoli provide evidence of this regression. Subsequent to this, there was a progressive sea level rise, possibly from the Early Holocene up to 6.0 ka BP, reaching a maximum level of 6 m above the present sea level around 3.0 ka BP.

Palaeoplain	Age	Process/lithology
	Mid-/Early-Holocene	Sea level 1.5-2.5 m below MSL/Clays with carbonized plant remains/Colva fossil wood
	Late-Pliocene/Pleistocene	Low sea level (60-90 m below MSL), shelf- edge ridges, rapid rise in sea level, river terraces, Sea-Level Laterites, Coastal Laterites
Mopa-Verna	Mid-Miocene/Early Pliocene	Low-Level Laterites
	Mid-Miocene	Transgressive cycle/shales with carbonaceous streaks e.g. Ratnagiri carbonaceous shales
Unconformity		
Mollem	Late Oligocene/Early Miocene	Intermediate-Level Laterites
	Late Oligocene	Seaward tilt with marine transgression
	Unconformity	
	Early Oligocene	Downwarping of the crust, submergence of Bombay High platform
	Late Eocene	Marine transgression Tarapur and Telwa shales
Unconformity		
Anmode	Mid Eocene	In-land lagoon Formation/change in drainage/ dissection of High-Level laterites/continental sediments-organic black shales e.g. Cambay shales
	Late Palaeocene/Early Eocene	Partly inland partly offshore basin Formation/terrigenous clastics on eastern flank of Laccadive ridge, High-Level Laterites

Table No. 2 Summary of the geomorphological evolution of Goa (after Dessai 2018)

## **LITERATURE REVIEW**

Nigam and Hashimi (1995) provided an overview of marine sediments and paleoclimatic variations that occurred in the Arabian Sea since the Late Pleistocene. Shetye et al. (2007) examined the environmental conditions influencing the Mandovi and Zuari estuaries in Goa. Prajith et al. (2016) investigated the distribution, provenance, and early diagenesis of major and trace metals in sediment cores from the Mandovi estuary in Goa. Alagarsamy (2006) studied the distribution and seasonal variation of trace metals in surface sediments of the Mandovi estuary. Mörner (2017) analyzed coastal morphology and sea-level changes in Goa, over the last 500 years. Kessarkar et al. (2010) examined the nature and distribution of particulate matter in the Mandovi estuary. Bhaskar et al. (2012) investigated the sedimentation of particulate matter in the Dona Paula Bay in Goa during the period from November to May 1995-1997. Rao (1974) characterized the textural characteristics of sediments in Mormugao Bay,. Chandramohan et al. (1998) studied fine particle deposition at Vainguinim tourist beach in Goa. Chaubey et al. (1993) contribute significant insights into the spreading history of the Arabian Sea, presenting novel constraints that enrich our understanding of its geological evolution. Hegde et al. (2021) delve into the granulometric dynamics of coastal sediments along the Central West coast of India, elucidating the interplay of morpho-tectonic factors in shaping beach processes, thus advancing our knowledge in this field.

# **CHAPTER III – METHODOLOGY**

## GEOLOGY OF THE STUDY AREA

Latitude: 15°27'51"N

Longitude: 73 ° 48'17"E

Caranzalem beach, extending approximately 2 km along the left bank of the Mandovi River, forms a bay-side beach, shielded by headlands, specifically Aguada to the north and Cabo Niwas to the south. A densely populated stretch is found at Campal, Miramar and Caranzalem. About 30 to 90m wide, the beach extends about 3.5 km southwards and terminates against the hill slopes of Dona Paula promontory. Caranzalem beach is partially protected from low swell waves in fair weather and high wind waves during the monsoon season. Caranzalem experiences low swell waves from the W to NW lasting 5-7 seconds during fair weather, and high wind waves from the W to SW with periods of 7-12 seconds during the monsoon. (Reddy, 1970). The northern end of Caranzalem beach is backed by natural features such as casuarina plantations and coconut groves, while a sea wall provides additional protection on the southern side. Caranzalem beach is subject to changes in water level due to semidiurnal tides, experiencing a range of 2m during spring tide. The country rock is encountered at 26.5m and megascopically it appears to be a metagreywacke belonging to the Sanvordem formation. The estuarine region is characterized by monsoon induced seasonal changes in physical, chemical and biological features (Qasim and Sengupta, 1981).

According to report, in contrast to Miramar, Caranzalem beach is characterized by a very flat and wider expanse, measuring about 200m. (Sonak, 2017)

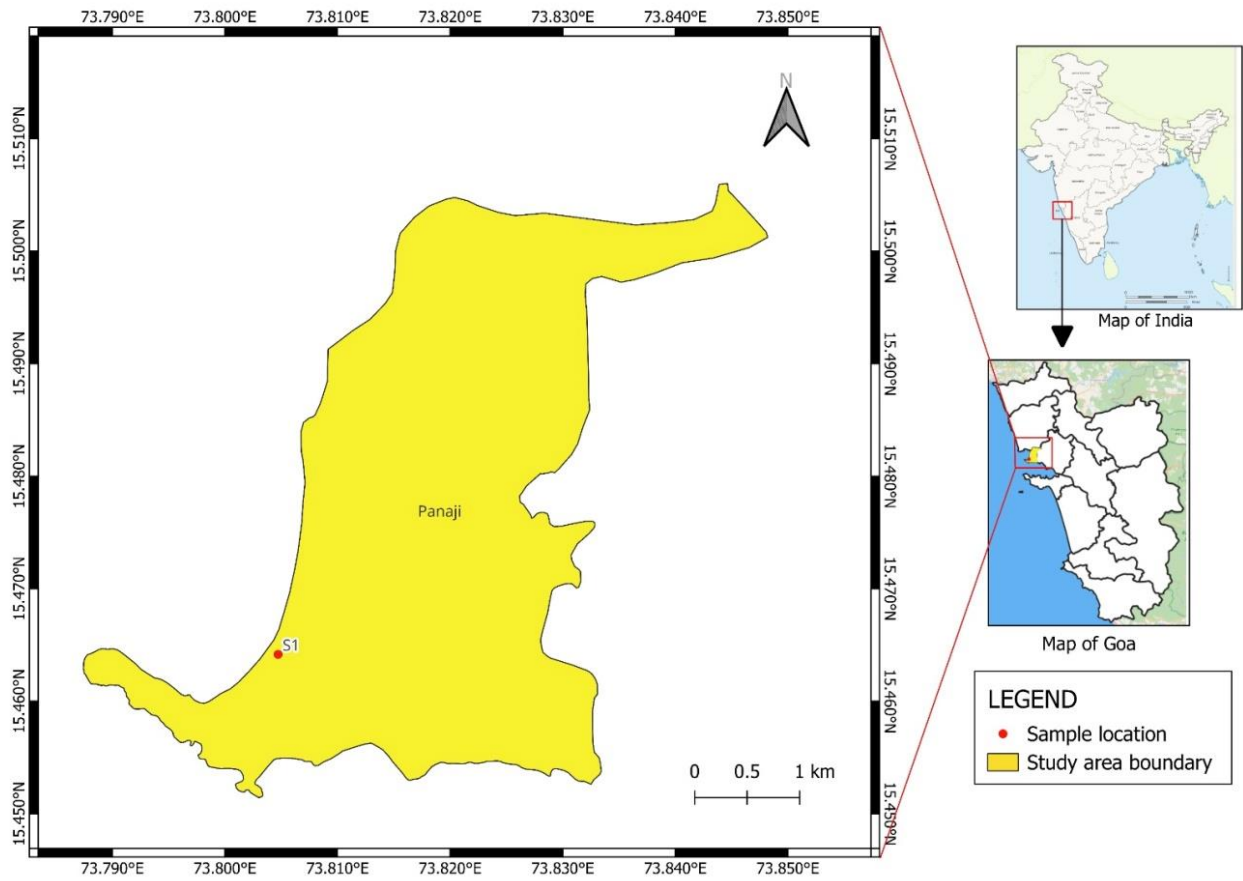


Figure No. 2 Study area map

## **GRAIN SIZE**

Sediments encompass solid inorganic or organic fragments resulting from rock weathering and soil erosion. Transported by wind, water, or ice, these particles, ranging from large blocks to microscopic entities, undergo deposition. Scientifically, sediment classification follows a size gradient, spanning boulders, cobbles, gravel, sand, silt, and clays.

Sediments arise through the disintegration of rocks, primarily transported by water, undergoing abrasion that rounds particles, diminishing sharp edges. Those resulting from land erosion are predominantly lithogenous sediments. Scientifically, the term "clastic" refers to sediments or sedimentary rocks comprised of fragments (detritus) from older rocks. "Clast" denotes a rock fragment, originating from the Greek "klastos," meaning broken. Examples include gravel, sand, and silt. The majority of lithogenous sediments can be classified as clastic.

Grain size is the average diameter of clasts (particles) of clastic sediments and rocks. Grain size is the primary parameter in sedimentary geology to divide clastic rocks and sediments in different classes for classification purposes. This subdivision is based on the Udden-Wentworth scale, which differentiates four major classes of sediments (and corresponding sedimentary rocks) that are further divided in sub-classes:

– gravel or ruditic grain size ( $> 2$  mm), which includes pebbles (2 – 64 mm), cobbles (64 – 258 mm) and boulders ( $> 258$  mm).

The corresponding rocks are conglomerate and breccia (further differentiated based on roundness);

- sand or arenitic grain size (0.0625 – 2 mm) and the corresponding sandstone;
- silt or siltitic grain size (0.004 – 0.0625 mm) and the corresponding siltstone;
- clay or lutitic grain size (<0.004 mm), whose lithified counterpart is claystone

### **GRAIN SIZE SCALE**

The Udden-Wentworth scale, widely used in sediment description, ensures equal significance across gravel, sand, silt, and clay through a logarithmic progression.

This scale maintains a consistent ratio between grain sizes, with each subsequent size class being half as large as the preceding one, progressing from gravel to clay.

The scale's logarithmic nature, with sizes like ¼, ½, 1, 2, 4, and 8 millimeters, facilitates precise classification of sedimentary particles, enabling geologists to characterize sedimentary rock formations accurately.

The Udden-Wentworth scale, widely adopted for sediment description, maintains equal significance across gravel, sand, silt, and clay by employing a logarithmic progression. Each subsequent size class is half as large as the preceding one (¼, ½, 1, 2, 4, 8... mm). Krumbein introduced the Phi scale, an arithmetic modification, expressed as  $\Phi$  units, with a logarithmic base. The conversion formula  $\Phi = -\log_2 d$  relates millimeter grain sizes (d) to Phi values. Phi values are dimensionless on this geometric scale. The particle size scale for clastic sediments and rocks uses Phi values, noting that an increase in Phi corresponds to a decrease in particle size. Notably, Phi values for grains coarser than one millimeter are negative, while those finer are positive.

PARTICLE LENGTH (d <sub>I</sub> )				GRADE	CLASS	FRACTION	
km	m	mm	φ			Unlithified	Lithified
1075				-30	very coarse	Megagravel	Mega-conglomerate
538				-29	coarse		
269				-28	medium		
134				-27	fine		
67.2				-26	very fine		
33.6				-25	very coarse		
16.8				-24	coarse		
8.4				-23	medium		
4.2				-22	fine		
2.1				-21	very fine		
1.0	1048.6			-20	very coarse	Slab	
0.5	524.3			-19	coarse		
0.26	262.1			-18	medium		
	131.1			-17	fine		
	65.5			-16	very coarse	Block	
	32.8			-15	coarse		
	16.4			-14	medium		
	8.2			-13	fine		
	4.1	4096		-12	very coarse	Boulder	
	2.0	2048		-11	coarse		
	1.0	1024		-10	medium		
	0.5	512		-9	fine		
	0.25	256		-8	coarse	Cobble	Gravel
		128		-7	fine		
		64		-6	very coarse	Pebble	Conglomerate
		32		-5	coarse		
		16		-4	medium		
		8		-3	fine	Granule	
		4		-2			
		2		-1	very coarse	Sand	Sand
		1		0	coarse		
		0.50		1	medium		
		0.25		2	fine		
		0.125		3	very fine	Silt	
		0.063		4	coarse		
		0.031		5	medium		
		0.015		6	fine		
		0.008		7	very fine	Clay	Mudstone or Shale
		0.004		8			
		0.002		9			
		0.001		10			
		0.0005		11			
		0.0002		12			
		0.0001		13			
					↓		
					?		

Table No:3 Modified Udden Wentworth grain size scale

## MEASURING GRAIN SIZE

The grain size of clastic sedimentary rocks serves as a crucial textural characteristic, providing insights into the source rock nature, transportational medium characteristics, sorting, depositional history, and tectonics of the depositional basin.

For unconsolidated sediments, manual measurements of boulders, cobbles, and pebbles employ calipers or tape. Granules to silt-size particles are commonly measured through sieving using nested wire-mesh screens. Mechanically shaken standard sieves of different mesh sizes capture particle size ranges, and the trapped material in each sieve is weighed. Finer sediments like silt and clay are measured using elutriation, where a sample treated with a dispersant settles in a cylinder, and the grain size is determined based on settling rates.

Methods of measuring sediment grain size		
Type of sample	Sample grade	Method of analysis
Unconsolidated sediment and disaggregated sedimentary rock	Boulders Cobbles Pebbles	Manual measurement of individual clasts
	Granules Sand Silt	Sieving, settling-tube analysis, image analysis
	Clay	Pipette analysis, sedimentation balances, photohydrometer, Sedigraph, laser-diffractometer, electroresistance (e.g., Coulter counter)
Lithified sedimentary rock	Boulders Cobbles Pebbles	Manual measurement of individual clasts
	Granules Sand Silt	Thin-section measurement, image analysis
	Clay	Electron microscope

Table No:4 methods of measuring sediment grain size

Stokes Law is applicable exclusively to particles categorized as very fine-grained, specifically sand-sized and finer. It operates under low Reynolds numbers, ensuring laminar flow during settling. However, the dynamics of particle descent undergo notable changes at higher Reynolds values, affecting particles of all shapes. In sedimentology, two crucial conditions to consider are flow separation and the motion of settling particles.

Stokes' law is valid under the following conditions.

- Particles must be solid, smooth, and spherical.
- Particles must be of uniform density.
- Particles must be sufficiently large ( $>0.001\text{mm}$ ) as compared to molecules of fluid so that the thermal (Brownian) motion of the fluid molecules does not affect the particles.
- Particles should not interfere with each other during the fall.
- The suspension should not have any turbulence, i.e., the flow must be laminar.

## X-ray Diffraction

X-ray diffraction has become a widely used method for studying crystal structures and atomic spacing, relying on the constructive interference of monochromatic X-rays with a crystalline sample. The X-rays, generated by a cathode ray tube, are filtered to produce monochromatic radiation, collimated for concentration, and directed towards the sample.

The incident X-rays interacting with the sample produce diffracted rays, following Bragg's law. These diffracted X-rays are then detected, processed, and counted. Scanning the sample through a range of angles covers all possible diffraction directions due to the random orientation of powdered material. Converting diffraction peaks to d-spacings facilitates compound identification since each compound has unique d-spacings. Typically, this involves comparing d-spacings with standard reference patterns.

The X-ray wavelengths are characteristic of the target material (Cu, Fe, Mo, Cr). Filtering, by foils or crystal monochrometers, is required to produce monochromatic X-rays needed for diffraction.  $K\alpha_1$  and  $K\alpha_2$  are sufficiently close in wavelength such that a weighted average of the two is used. Copper is the most common target material for single-crystal diffraction, with  $CuK\alpha$  radiation = 1.5418 Å. These X-rays are collimated and directed onto the sample. As the sample and detector are rotated, the intensity of the reflected X-rays is recorded. When the geometry of the incident X-rays impinging the sample satisfies the Bragg Equation, constructive interference occurs and a peak in intensity occurs. A detector records and processes this X-ray signal and converts the signal to a count rate which is then output to a device such as a printer or computer monitor.( Bunaciu,et.al,2015) . The interaction

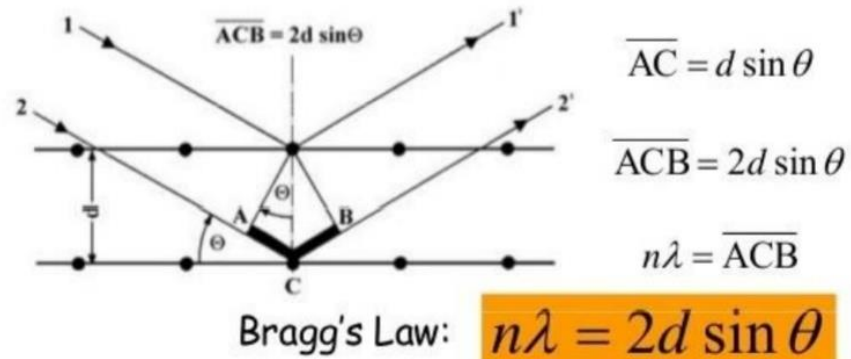
of the incident rays with the sample produces constructive interference (and a diffracted ray) when conditions satisfy Bragg's Law. This law relates the wavelength of electromagnetic radiation to the diffraction angle and the lattice spacing in a crystalline sample. These diffracted X-rays are then detected, processed and counted. By scanning the sample through a range of  $2\theta$  angles, all possible diffraction directions of the lattice should be attained due to the random orientation of the powdered material. Conversion of the diffraction peaks to d-spacings allows identification of the material because each material has a set of unique d-spacings. Typically, this is achieved by comparison of d-spacings with standard reference patterns.

### **Bragg's Law**

Bragg showed that if the diffraction from a crystal was considered as reflections from imaginary planes of atoms within the crystal then an equation could be formulated to predict where diffraction maxima would occur in a diffraction pattern. Considering a pair of parallel X-rays striking a pair of horizontal parallel planes. The parallel rays hit the planes in phase but the lower ray has a longer distance to travel than the upper one by the time they are both reflected. By simple trigonometry it can be shown that  $n\lambda = 2d\sin\theta$ . The Bragg relationship shows that constructive interference of the waves will only occur when the path difference is some multiple of the wavelength,  $\lambda$ .

Bragg observed that, unlike the reflection of ordinary light, X-ray reflection specifically occurs at certain angles determined by the wavelength of the X-rays and the interplanar distance within the crystal lattice. Two notable geometric principles include: (1) the incident beam, the normal to the reflecting plane, and the diffracted

beam always lie in the same plane, and (2) the angle between the diffracted beam and the transmitted beam is consistently ( $2\theta$ ), referred to as the diffraction angle, which is the angle typically measured experimentally rather than ( $\theta$ ).



### Powder X-ray diffraction (PXRD)

Powder X-ray diffraction (PXRD) is perhaps the most widely used analytical technique for characterizing materials. As the name suggests, the sample is usually in a powdery form, consisting of fine grains of single crystalline material to be studied. The technique is also used widely for studying particles in liquid suspensions or polycrystalline solids (bulk or thin film materials). The term 'powder' really means that the crystalline domains are randomly oriented in the sample. Therefore when the 2-D diffraction pattern is recorded, it shows concentric rings corresponding to the various  $d$  spacings in the crystal lattice.

The positions and the intensities of the peaks are used for identifying the underlying structure (or phase) of the material. A powder XRD scan typically represents a plot of scattering intensity v/s. the scattering angle  $2\theta$  or the corresponding  $d$ -spacing.

### **Components Of Diffractometer Are**

- X-ray Tube: the source of X Rays.
- Incident-beam optics: to condition the X-ray beam before it hits the sample
- Goniometer: the platform that holds and moves the sample, optics, detector, and/or tube
- Sample holder
- Receiving-side optics: to condition the X-ray beam after it has encountered the sample
- Detector: to count the number of X Rays scattered by the sample.

Applications of X-ray diffraction encompass determining unit cell dimensions, identifying composite materials with multiple crystallographic phases and quantifying each phase's fraction. It is valuable for distinguishing between crystalline and amorphous materials, determining grain/particle size, assessing the degree of texture and polygrained materials, measuring sample purity, as well as determining the orientation of single crystals. Additionally, X-ray diffraction plays a role in understanding electron distribution within atoms, characterizing molecular structures, and analyzing proteins and nucleic acids.

### **The Munsell Chart**

The Munsell System, developed by Albert H. Munsell, is a color classification system based on three variables: hue (color name), value (lightness or darkness), and chroma (purity or difference from neutral gray). Each color is identified with an alphanumeric label representing these three variables. What sets Munsell apart is the

independence of these variables; if two colors share one variable, they appear the same in that aspect even if the other two variables differ.

Munsell experimented by changing one variable at a time to create scales of colors that change at a perceptually uniform rate. He organized the color samples into a three-dimensional solid shape with hue, value, and chroma as axes. Unlike other systems of the time, Munsell's color solid was irregularly shaped, reflecting the unique relationships between hue, chroma, and value. This innovation accurately mapped the nuances of human color perception, departing from the geometrically inspired shapes used in other color systems.

The Munsell color order system is a method for defining and communicating colors based on three key dimensions: hue, value, and chroma.

1. Hue: This dimension corresponds to the dominant wavelength of a color, essentially identifying the color family (e.g., red, blue, yellow). Hue is represented in the Munsell system in a circular arrangement.
2. Value: Value refers to the brightness or lightness of a color. In the Munsell system, it is represented on a vertical scale, with higher positions indicating lighter colors and lower positions indicating darker colors.
3. Chroma: Chroma measures the strength or purity of a color. It represents the intensity or vividness of a color. In the Munsell system, chroma is depicted radially from the center of the hue circle, with colors becoming more vivid as they move outward.

## **CLAY MINERALOGY**

The term “clay mineral” refers to phyllosilicate minerals and to minerals which impart plasticity to clay and which harden upon drying or firing. Clay minerals are layer silicates that are formed usually as products of chemical weathering of other silicate minerals at the earth's surface. Clay minerals resemble the micas in chemical composition, except they are very fine grained, usually under microscope. Like the micas, clay minerals are shaped like flakes with irregular edges and one smooth side. Clay minerals form an important group of the phyllosilicates or sheet silicate family of minerals, which are distinguished by layered structures composed of polymeric sheets of  $\text{SiO}_4$  tetrahedral linked to sheets of  $(\text{Al, Mg, Fe})(\text{O,OH})_6$  octahedral. The geochemical importance of clay minerals stems from their ubiquity in soils and sediments, high specific surface area, and ion exchange capacities. Clay minerals tend to dominate the surface chemistry of soils and sediments.

### **Clay Origin**

The formation, alteration, and accumulation of clay minerals are complex processes influenced by a diverse array of environmental factors. Predominantly, these processes are mediated by the chemical reactions and physical transport facilitated by water. Consequently, clay minerals emerge as prominent constituents within Earth's near-surface hydrous environments, spanning weathering, sedimentation, diagenesis/low-grade metamorphism, and hydrothermal alteration regimes. Within these contexts, clay minerals serve as indicators of the intricate interplay between geological, atmospheric, and biological processes, highlighting their pivotal role in shaping terrestrial landscapes.

The weathering environment delineates the realm wherein rocks and their mineral constituents undergo modification under the influence of atmosphere, hydrosphere, and biosphere agents. Concurrently, soil formation, or pedogenesis, manifests as a dynamic process within the weathering environment. The sedimentary environment represents the locus wherein the erosive forces of water, wind, and ice facilitate the transport and deposition of soil, weathered rock, and mineral particles, alongside biogenic materials. Diagenesis encompasses the suite of physical and chemical transformations occurring between sedimentation and metamorphism, while hydrothermal alteration denotes the intricate interactions between heated water and rock matrices, elucidating the multifaceted nature of clay mineral genesis and evolution.

There are three types of clay minerals:

- Kaolinite clay
- Montmorillonite clay
- Illite clay

All of these clay minerals have two basic atomic sheets

1. Silica tetrahedral sheet
2. Aluminum octahedron sheet

In silica tetrahedral sheet, silica (Si) occupies the center positions and oxygen ions (O) are strongly bonded to the core atoms. Silica tetrahedral sheet is symbolized with a trapezoid, of which the shorter face holds electrically unsatisfied oxygen atoms and the longer face holds electrically satisfied oxygen atoms.

(Kumari,N,2021)

In aluminum octahedron sheet, aluminum (Al) ion positioned at the center and hydroxyl ion (OH-) bonded to the core atoms. Aluminum octahedron sheet is symbolized with a rectangle with top and bottom faces having the same characteristics of exposed hydroxyl ions.

### **Kaolinite**

Kaolinite, the main constituent of kaolin, is formed by rock weathering. It is white, greyish-white, or slightly coloured. It is made up of tiny, thin, pseudo-hexagonal, flexible sheets of

triclinic crystal with a diameter of 0.2–12  $\mu\text{m}$ . It has a density of 2.1–2.6  $\text{g/cm}^3$ .

Upon heating, kaolinite starts to lose water at approximately 400 °C, and the dehydration approaches completeness at approximately 525 °C (Grim, 1968). The dehydration depends on the particle size and crystallinity. Kaolinite consists of trioctahedral minerals such as , chrysotile, chamosite, and antigorite as well as similarly dioctahedral minerals such as halloysite, kaolinite, nacrite, and dickite. This clay is usually white and has a soft plastic-like texture. It is composed of hydrated aluminum silicate and mineral kaolinite.

### **Montmorillonite**

Montmorillonite, a type of smectite mineral, is an aqueous aluminum silicate. It has a layered crystalline structure with the general chemical formula of  $(\text{Na,Ca})\cdot(\text{Al, Mg})\cdot(\text{SiO})\cdot(\text{OH})\cdot n\text{H}_2\text{O}$ . ( H.Ciftci,2021). Rocks that mostly contain montmorillonite mineral are also called as bentonite.

Montmorillonite clay has some superior characteristics such as high surface area, high swelling capacity, good adsorbent ability, high cation exchange capacity, plasticity, high chemical stability, and good mechanical properties. It has a high swelling capacity when hydrated.

### **Illite**

Illite, belonging to the mica-type clay mineral group, is extensively found in marine shales and associated sedimentary deposits. Characterized by a mica like sheet structure, illite possesses a composition with relatively higher water content and lower potassium content compared to true micas. Despite its resemblance to micas, illite exhibits a poorly crystallized nature. It often participates in a chemical series alongside muscovite and montmorillonite, indicative of its transitional properties between these minerals. Illite is a non-swelling clay mineral that is commonly found in sedimentary rocks. Illite emerges as a product of weathering processes acting upon muscovite, and it undergoes alteration into montmorillonite particularly under humid environmental conditions.

.

.

## **SAMPLING**

Borehole retrievals were obtained from Rajdeep builders Project at Caranzalem.

### **Sample Preparation**

Approximately 25 grams of each sample (totaling 8 samples) were weighed into individual 250 mL beakers. A small amount of water was added to each beaker, and the samples were allowed to soak. Following soaking, the samples were gently crushed using a glass rod. Subsequently, 100 mL of 6% hydrogen peroxide solution was added to each sample with continuous stirring and heated to 40°C for one hour. After heating, sediments were permitted to settle, and the supernatant was decanted to the minimum level. The samples were then washed with distilled water.

Next, 40 mL of 2M sodium carbonate solution was added to each sample with continuous stirring, and the sediments were allowed to settle. The supernatant was decanted, and the samples were washed with distilled water 3-4 times. This process aimed to remove organic matter, silica content, and salinity from the samples. The saline-free samples were decanted to a minimum water level, and 1-2 mL of 10% sodium hexametaphosphate was added to each sample, followed by stirring and a resting period of at least 2 hours.

Afterward, the samples were decanted, separating the sand fraction which was gathered in preweighed 100 mL beakers and transferred to an oven for drying. The separated sample solutions were then collected into a 1-liter measuring cylinder, stirred well, and allowed to settle without disturbance.

Samples of 20 mL were pipetted out after specific time intervals (20 seconds, 4 minutes 28 seconds, and 3 hours 41 minutes) from depths of 20 cm, 10 cm, and 5 cm, respectively. These samples were collected in pre-weighed beakers and placed in an oven for drying. After drying, the beakers were weighed for grain size

calculations. Finally, the samples were further ground for X-ray diffraction (XRD) analysis.



Figure No. 3: samples kept for soaking



Figure No. 4: Sample sterilised from organisms



Figure No. 5: Samples kept for settling in 1000 ml volumetric cylinder



Figure No. 6: 10 ml pipetted out for XRD



Figure No.7: Samples kept for drying

### **X-Ray Diffractometer Rigaku Smartlab**

The SmartLab SE represents a highly adaptable and multifunctional X-ray diffractometer featuring built-in intelligent guidance capabilities. It embodies a refined iteration of the user-friendly design principles that earned its predecessor, the SmartLab, the R&D 100 Award in 2006, incorporating features such as automatic alignment, component recognition, cross-beam optics, and advanced photon counting hybrid pixel array detectors (HPAD). Key features include an architecturally integrated modular platform, facilitated by the SmartLab Studio 11 software, which leverages a novel cross-beam optics module enabling seamless

transitions between Bragg-Brentano and parallel beam configurations without the need for optic adjustments.

The inclusion of the HyPix-400 2D detector allows for effortless switching between 0D, 1D, and 2D detection modes, catering to diverse application requirements. Additionally, the D/tex Ultra 250 1D detector significantly accelerates powder diffraction processes, achieving a speed enhancement factor of 250 while offering adjustable energy resolution of approximately 20% or 4% contingent upon the sample under investigation.



Figure 8 & 9 : XRD machine, Smartlab X-ray Diffractometer from Rigaku at Goa University

# **CHAPTER IV- ANALYSIS AND CONCLUSIONS**

### GRAIN SIZE DATA

Sample Depth	Sample ID	SAND %	SILT %	CLAY %
8.78 m	1	73.94	0.15	26.75
12.14 m	2	93.90	0.41	6.1
14.99 m	3	93.75	0.052	6.1
18.06 m	4	94.8	0.008	1.29
21.06 m	5	92.86	0.002	6.89

Table No:5 Percentage of sediment fraction

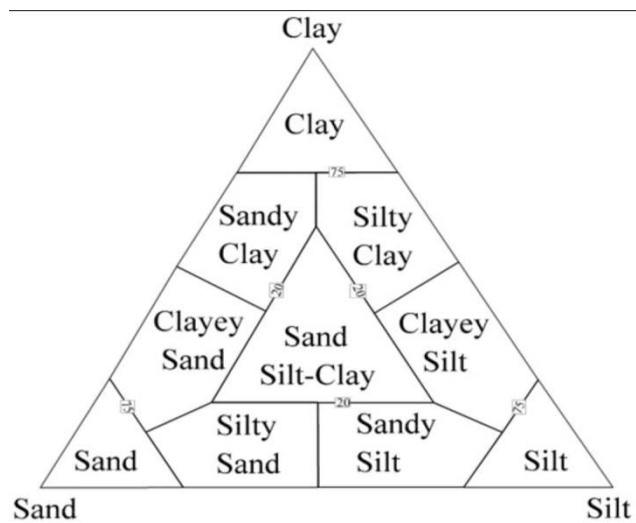
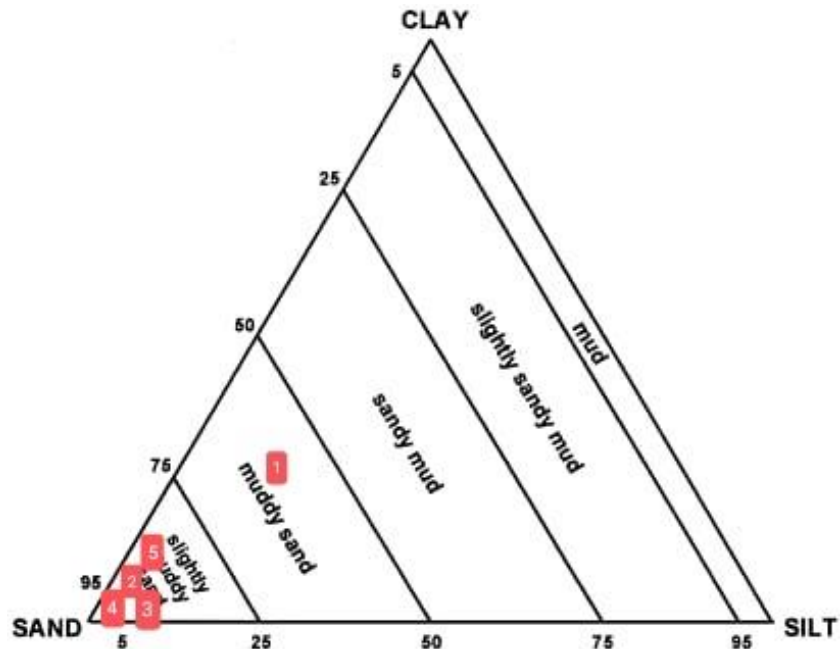


Figure No: 10 Diagram showing sand-silt-clay texture



Refer (table no.5)

Figure No: 11 Ternary diagram for sand-silt-clay mixture (after Flemming, 2000)

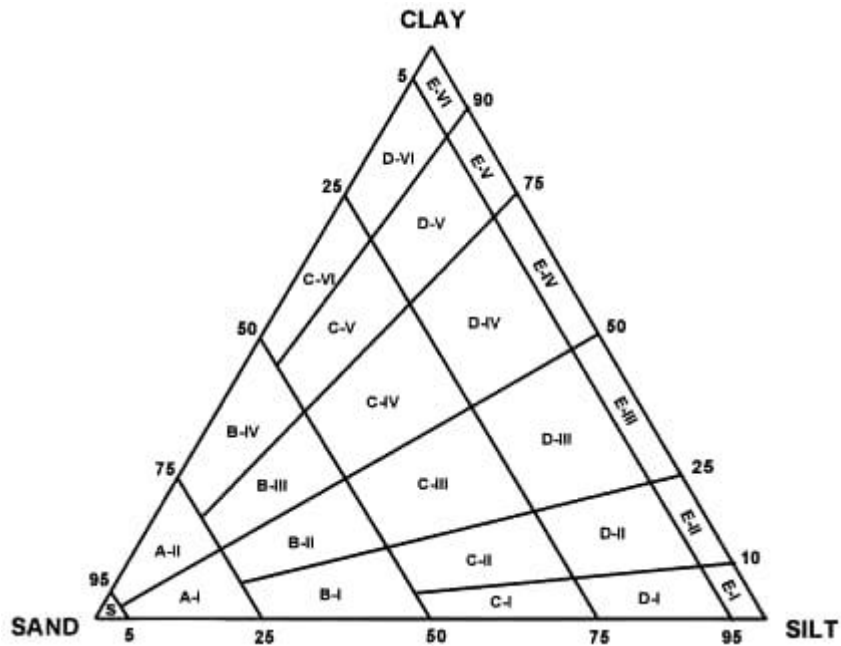
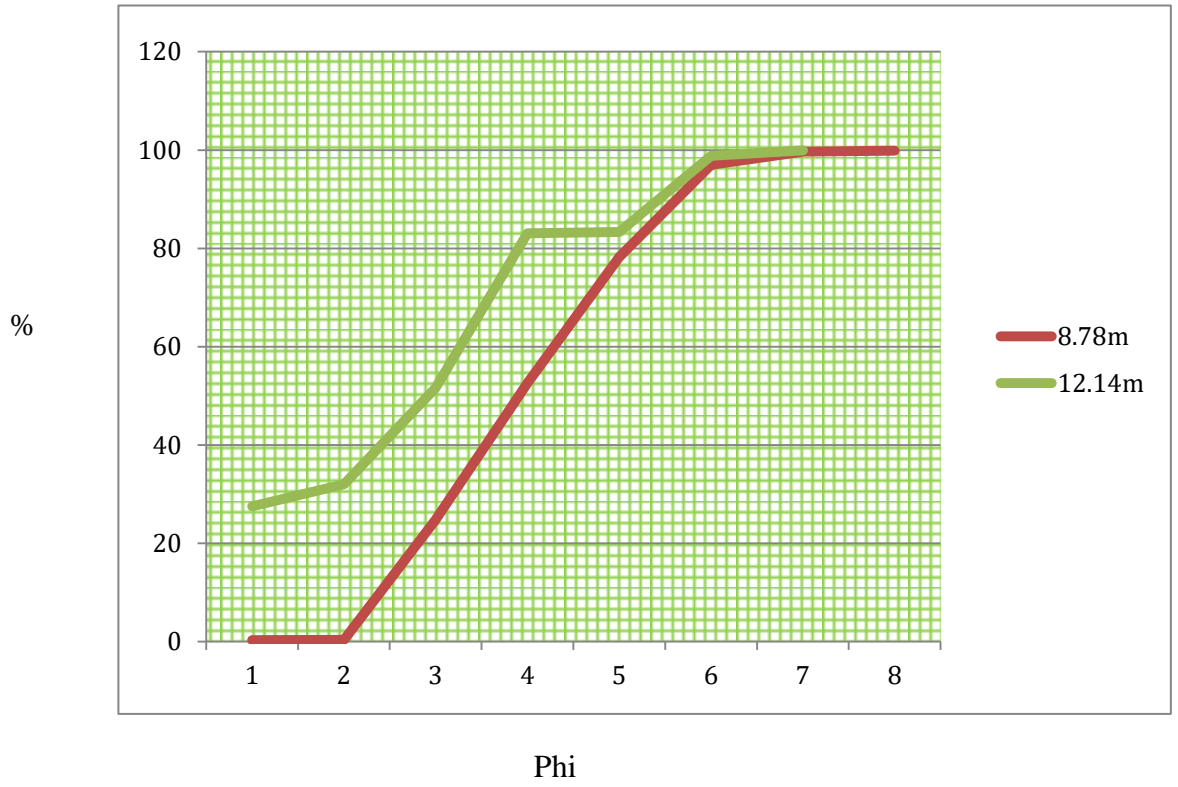


Figure No: 12 Ternary diagram for hydrodynamic condition (Perjup, 1988)

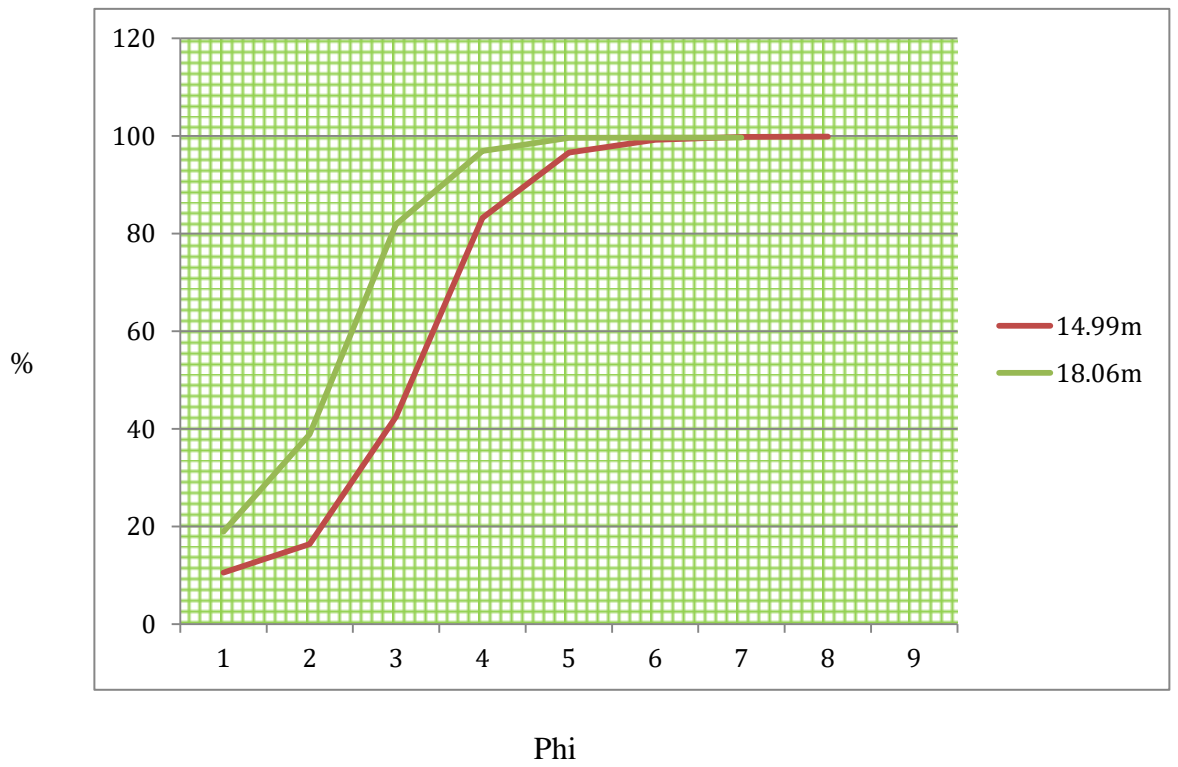
SAMPLE ID	CODE	TEXTURAL CLASS NAME
8.78m	1	MUDDY SAND
12.14m	2	SLIGHTLY MUDDY SAND
14.99m	3	SLIGHTLY MUDDY SAND
18.06m	4	SLIGHTLY MUDDY SAND
21.06m	5	SLIGHTLY MUDDY SAND

Table No: 6 Descriptive terminology of the three- component sand- silt- clay sedimentary system illustrated in graph no. 2 (after Flemming, 2000).

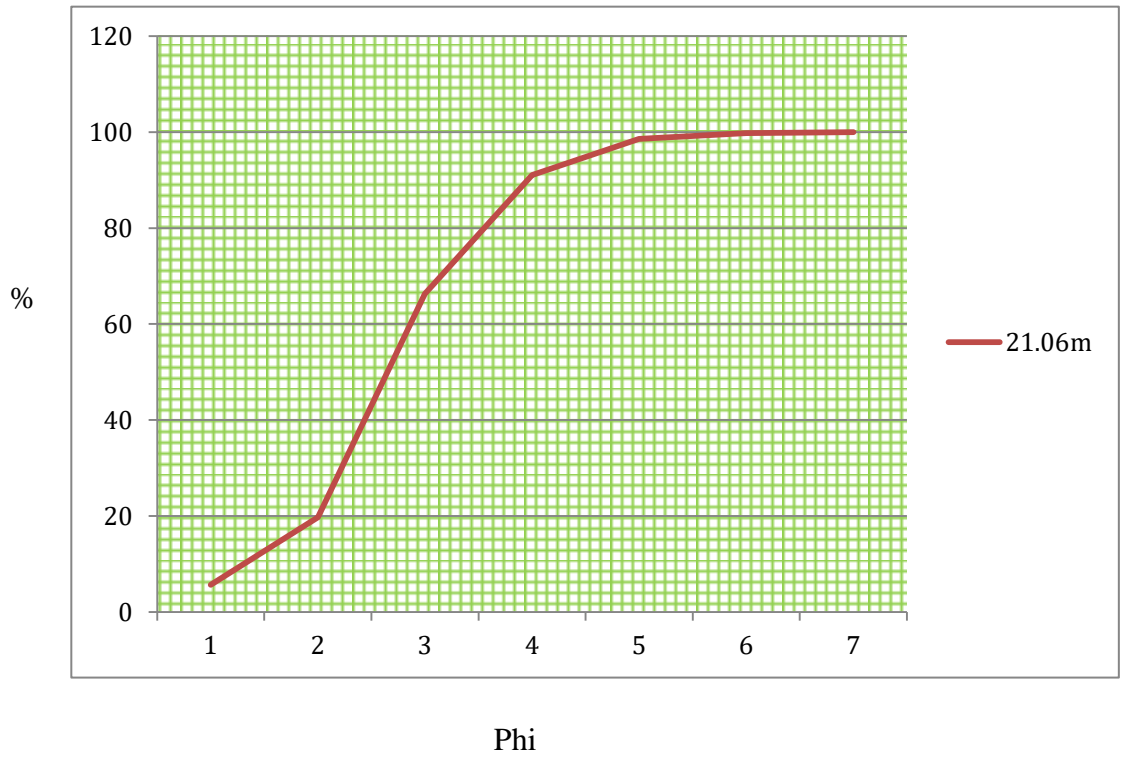
Graph No. 1



Graph No.2



Graph No.3



Graph No: (1)- (3) cumulative graph of sediment

Sample depth	Mean		Standard Deviation		Skewness		Kurtosis	
8.78 m	2.1	Fine	0.6	Moderately well sorted	0.083	Positive skewed	0.96	Mesokurtic
12.14 m	1.53	Medium	0.99	Moderately sorted	-01	Negatively Skewed	0.52	Very platykurtic
14.99 m	1.73	Medium	0.61	Moderately well sorted	-0.225	Negatively Skewed	1.2	Leptokurtic
18.06 m	1.1	Medium	0.62	Moderately well sorted	0.2	Positive skewed	1.02	Platykurtic
21.06 m	1.16	Medium	0.63	Moderately well sorted	0.288	Positive skewed	1.79	Very leptokurtic

Table No: 7 Graphical grain size parameters for sediment samples

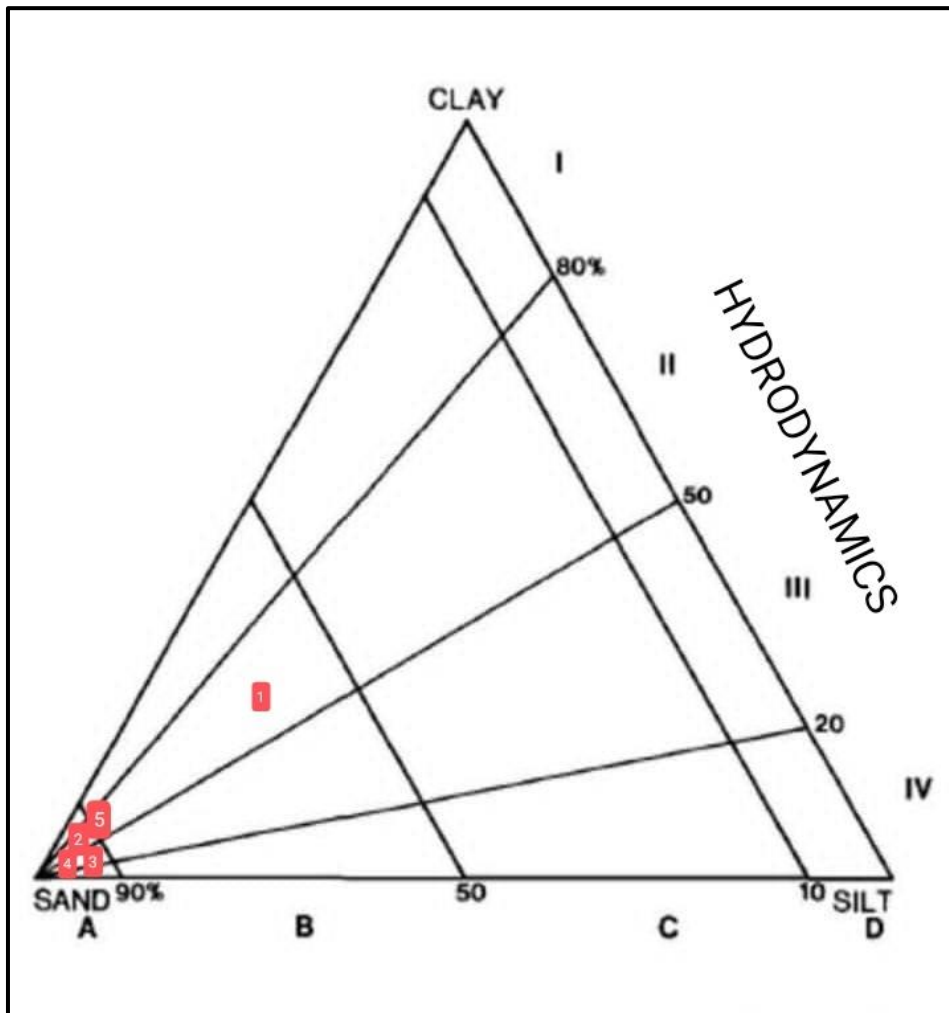


Figure No:13 Ternary diagram for classification of hydrodynamic conditions of depositional environment (after Perjup, 1998)

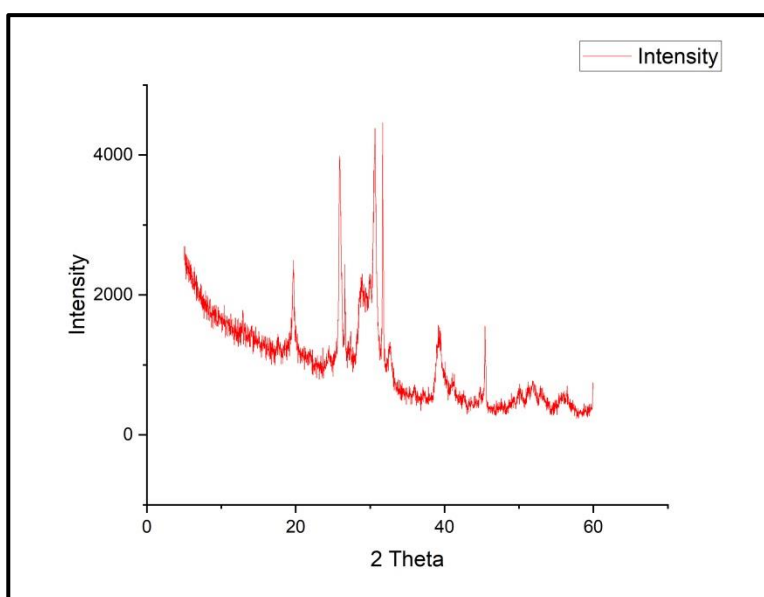
Table 5 provides a textural classification of each sample. In Table 6, the terms mean, standard deviation, skewness, and kurtosis are mentioned together with their values and descriptions. From 1 to IV, hydrodynamic conditions get more intense, according to the ternary diagram (Perjup 1998). As can be observed in figure no.14 Sample 2,3,4,5 that is (12.14m,14.99m, 18.06m, 21.06m respectively) fall under category IV, which had hydrodynamic conditions that were turbulent and strong and sample no.1 (8.78m) had hydrodynamic conditions that were moderately turbulent.

## CLAY MINERALOGY

X-ray diffraction patterns were obtained for 5 samples using Rigaku X-ray diffractometer with copper source. Sample slides were prepared and placed in the diffractometer. Each sample analysis took 15 minutes for analysis.

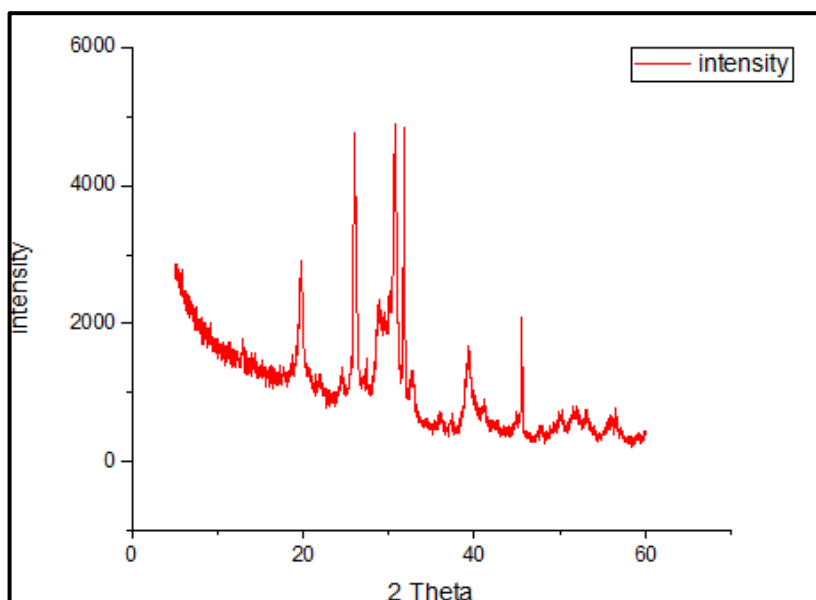
(1)

8.74 A



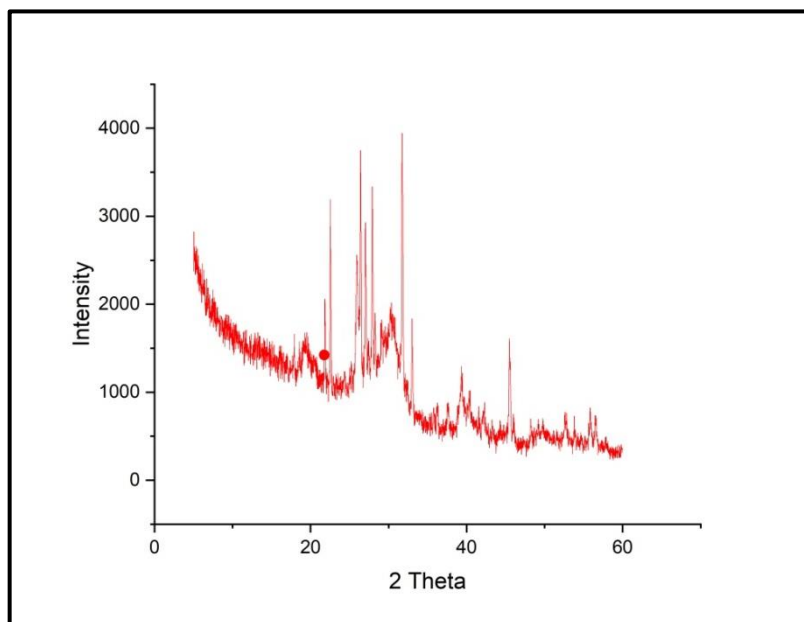
(2)

8.78 B



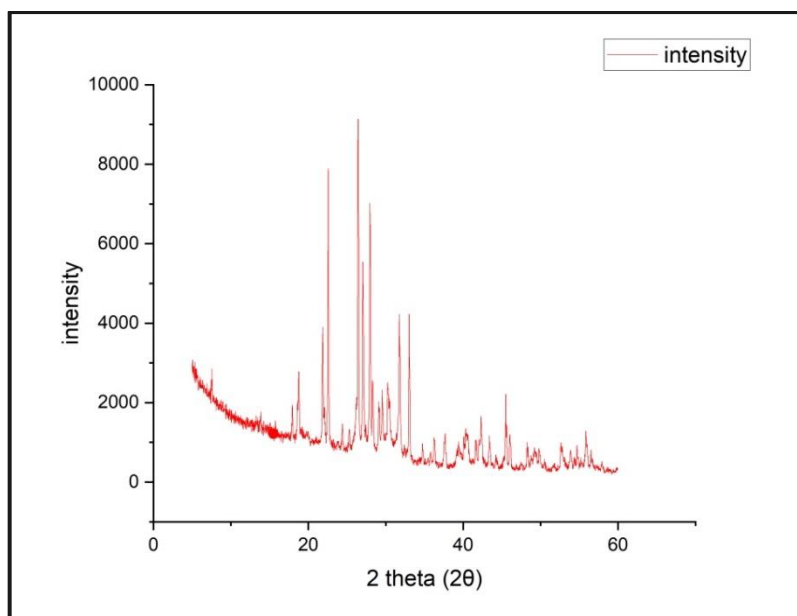
(3)

8.78 C



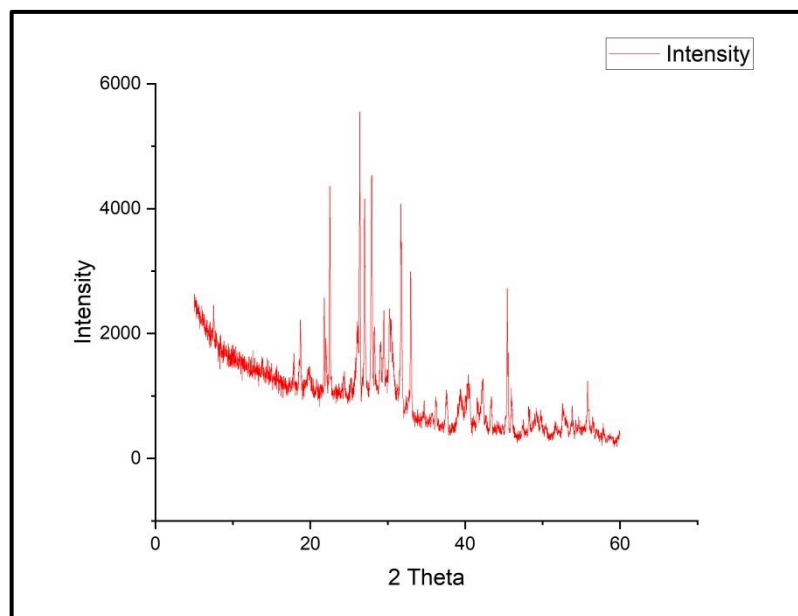
(4)

12.14 A



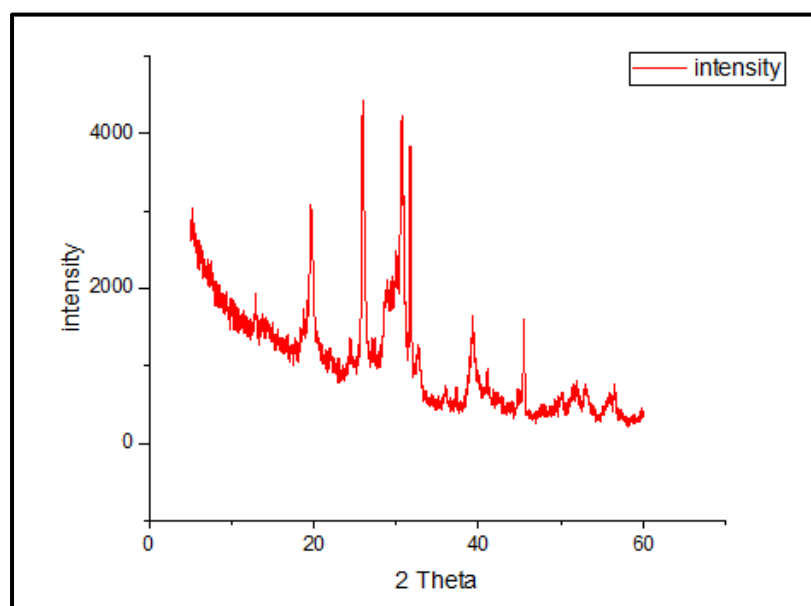
(5)

12.14 B



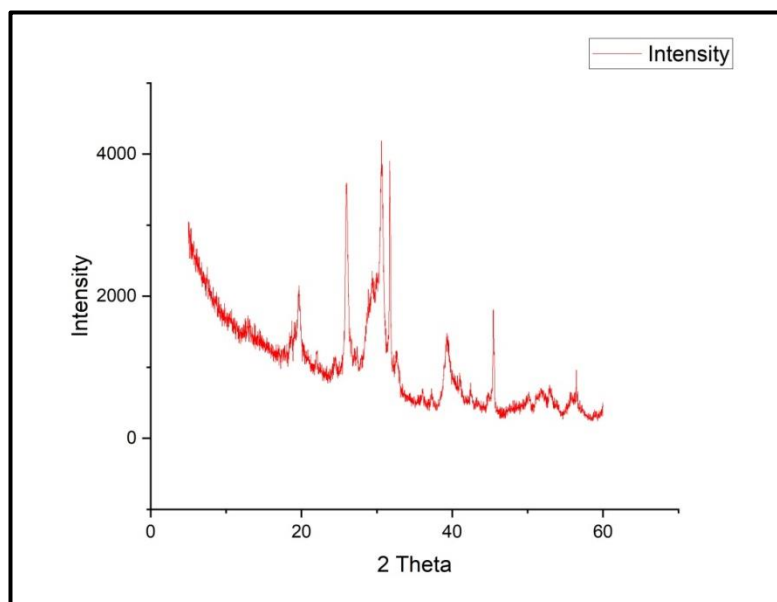
(6)

12.14 C



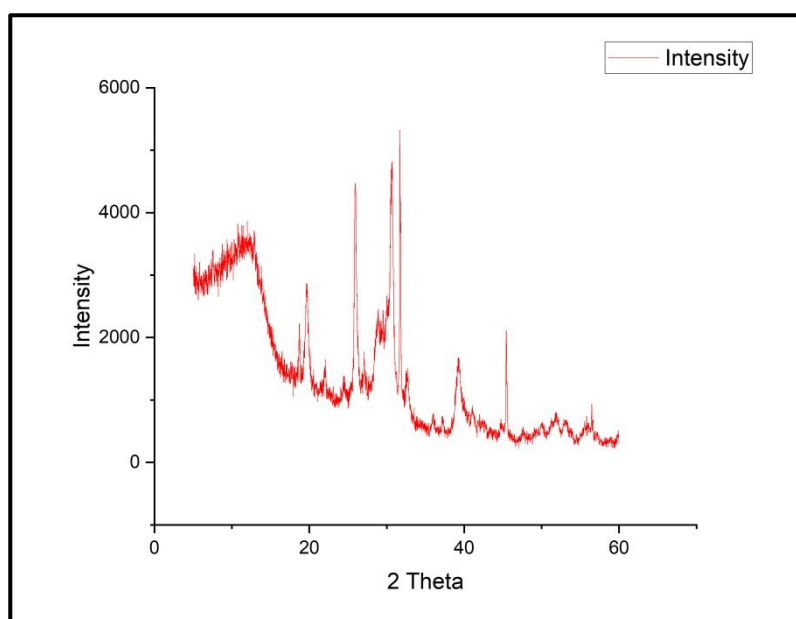
(7)

14.99 A



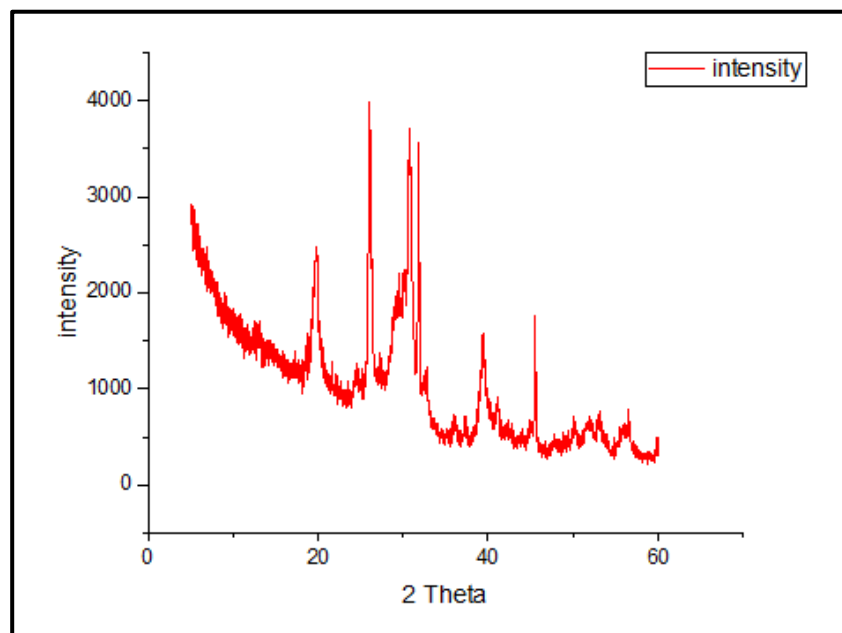
(8)

14.99 B



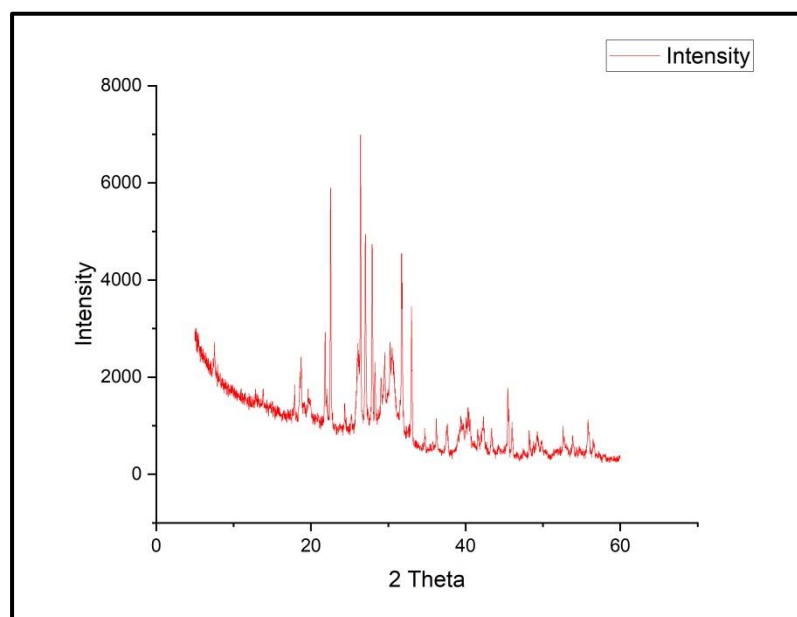
(9)

14.99 C



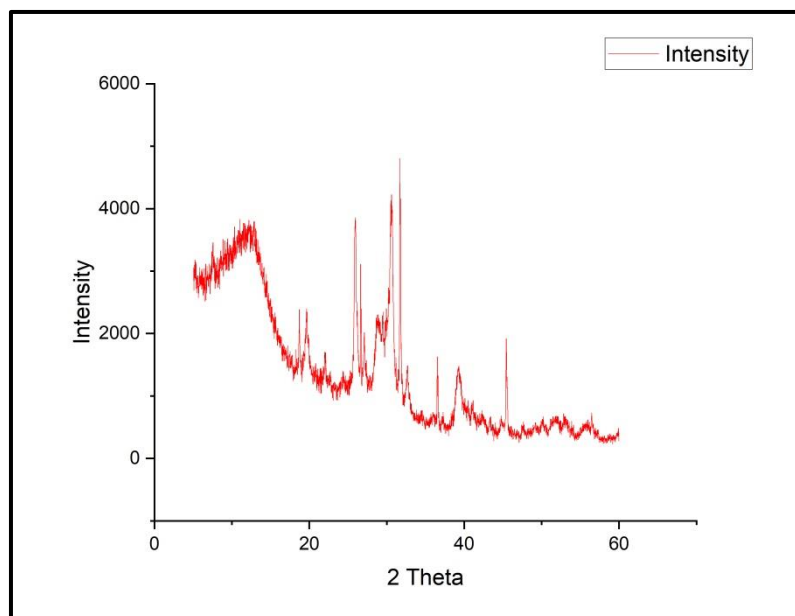
(10)

18.06 A



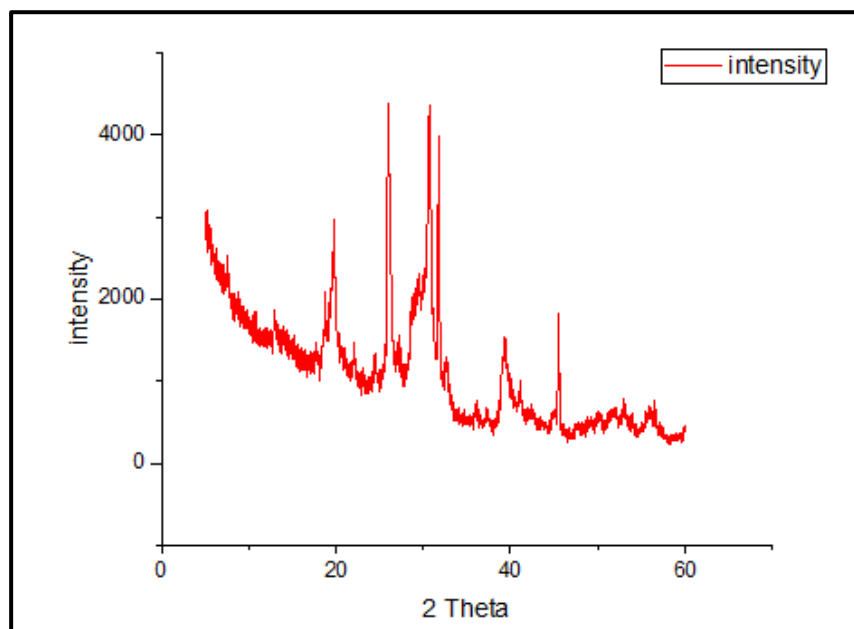
(11)

18.06 B



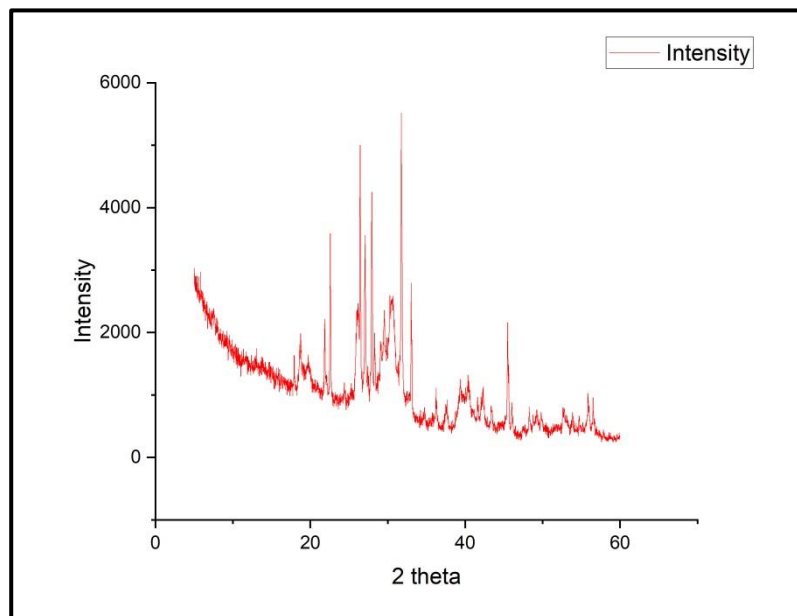
(12)

18.06 C



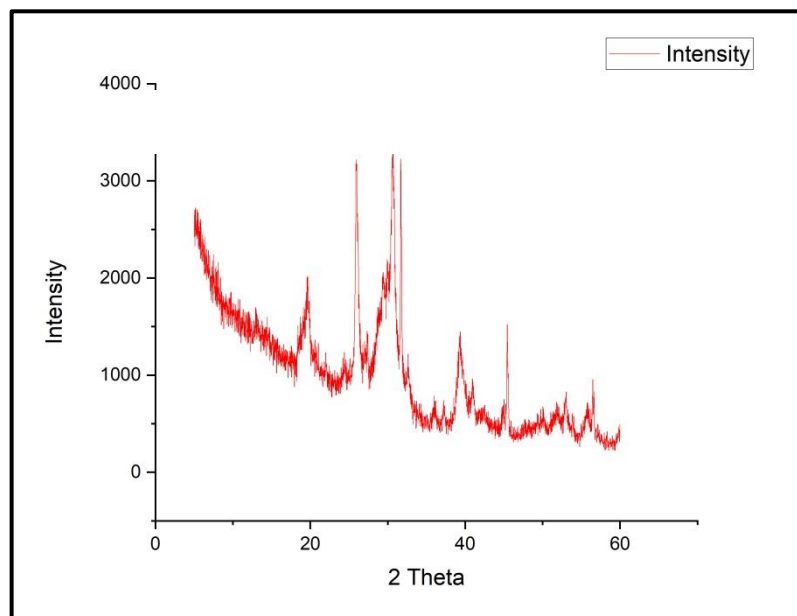
(13)

21.06A



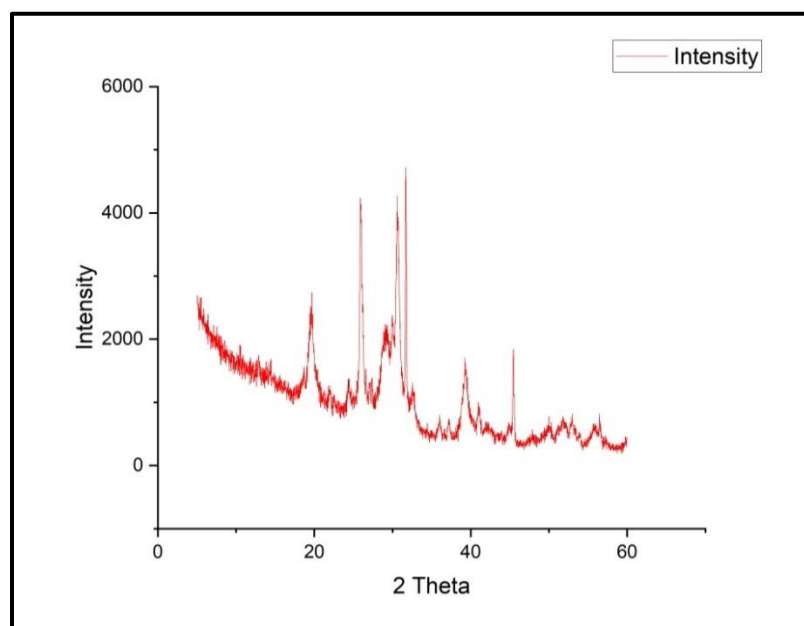
(14)

21.06 B



(15)

21.06 C

**Figure (1) – (15) Xrd pattern of samples**

SAMPLE ID	CLAY MINERALS
8.78m_A	Kaolinite, haematite, illite, quartz, goethite
8.78m_B	Kaolinite, haematite, illite, quartz, goethite
8.78m_C	Kaolinite, haematite, illite, quartz, goethite
12.14m_A	Kaolinite, haematite, illite, quartz
12.14m_B	Kaolinite, haematite, illite, quartz
12.14m_C	Kaolinite, haematite, illite, quartz
14.99m_A	Kaolinite, haematite, illite, quartz, goethite
14.99m_B	Kaolinite, haematite, illite, goethite
14.99m_C	Kaolinite, haematite, illite, quartz, goethite
18.06m_A	Kaolinite, haematite, illite, quartz
18.06m_B	Kaolinite, haematite, illite, quartz
18.06m_C	Kaolinite, haematite, illite, quartz
21.06m_A	Kaolinite, haematite, illite, quartz
21.06m_B	Kaolinite, haematite, illite, quartz
21.06m_C	Kaolinite, haematite, illite, quartz

Table No:8 Clay minerals depthwise

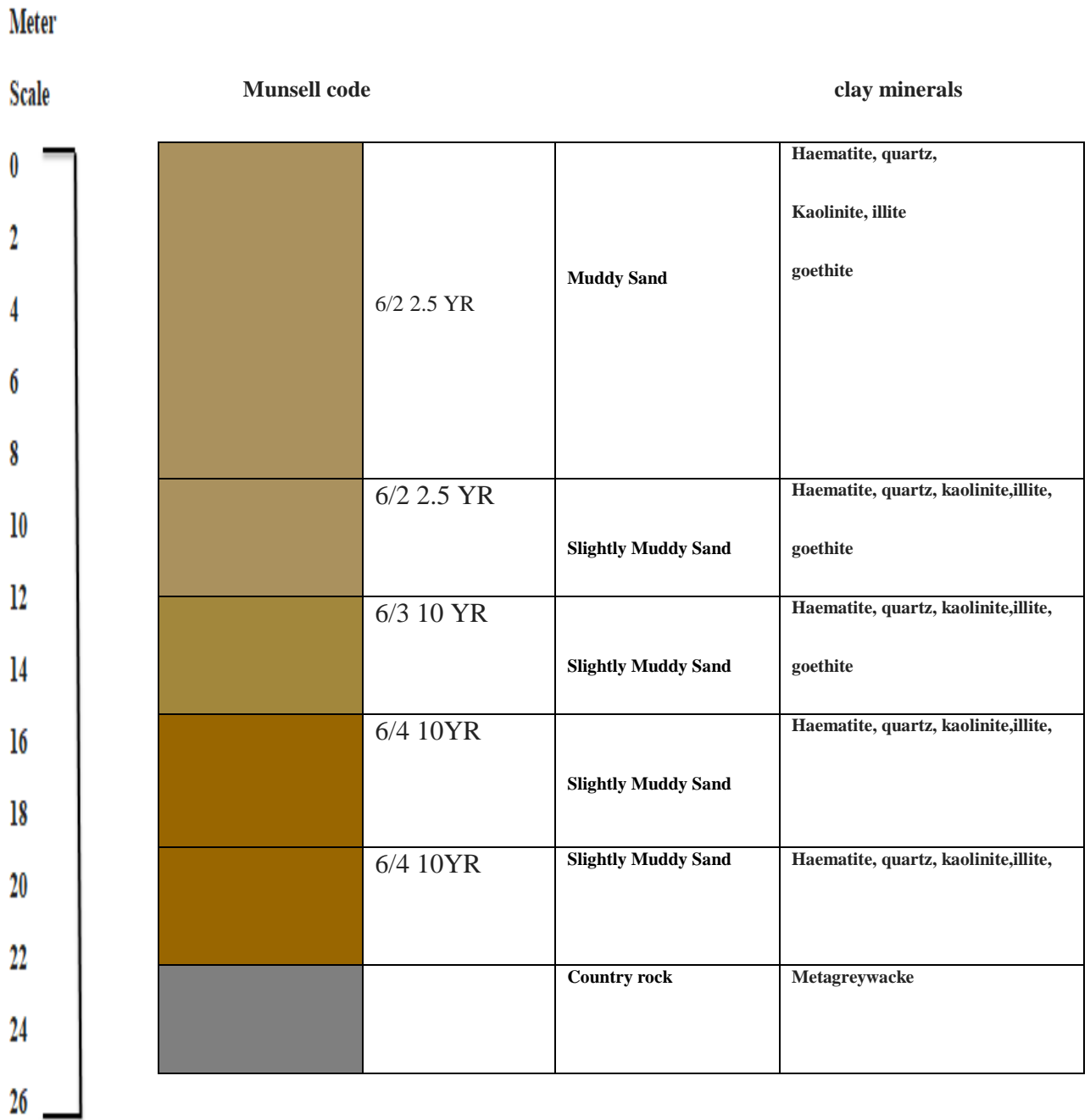


Figure No14. Lithology of study area

## INTERPRETATION

The study area constitutes river estuarine sediments and I used grain size analysis to determine the lithology, sediment mineralogy and sequence of depositional environments. Grain size vary from fine 2.1 at (8.78m) to medium 1.53,1.73, 1.1, 1.16 (table no.7), indicating different origins or transportation mechanism for the sediment. Finer grains owe their provenance from far away or calm areas. Medium sized grains come from nearby sources or more active environments. In terms of sorting, moderately well sorted 0.6 ,0.99, 0.61, 0.62 and 0.63 (table no.7 ) indicates fluctuations in energy levels of the river. Skewness spans from near symmetrical to strongly coarse or fine skewed , reflecting the distribution of grain sizes within sediment. The negatively skewed sands -01 and -0.225 (table no.7 ) are indicative of a turbulent state of the depositing medium, produced by the sudden drop in its energy and the positively skewed sands 0.083, 0.2, 0.288 ( table no.7) on the other hand indicate a relatively calm and steadily decreasing energy state of the depositing agent. Awasthi,(1970). Kurtosis ranges from mesokurtic to very platykurtic, depicting the shape of the sediment grain size distribution curve. Mesokurtic 0.96 (table no. 7) distributions indicate a normal distribution, while platykurtic 1.02 (table no. 7) ones are flatter with fewer extreme values, and leptokurtic 1.2 (table no .7 ) distributions have a higher peak and heavier tails, Very platykurtic 0.52 ( tableno.7) are extremely flat and spread out and Very leptokurtic 1.79 ( table no.7) are extremely peaked with heavier tails indicating an even higher probability of extreme values. Alterations in kurtosis signal fluctuations in sedimentation rates, depositional environments, or sediment sources.

Kaolinite, is commonly associated with weathering of aluminum-rich rocks, while quartz is abundant in various types of parent rocks. Illite, a type of clay mineral, forms through the alteration of other minerals and is often found in sedimentary environments.

### **Presence of haematite and goethite**

During monsoons, flooding in Mandovi estuary is believed to be caused by transfer of water from mining areas in the western region of Goa that transports iron ores (Gaonkar, et.al.2021). The entry of this water is associated with the presence of haematite and goethite in Mandovi estuarine sediments.(Shetye, et.al. 2007). Flooding events may thus relate to a connection between these minerals from iron ore alongside their introduction into the estuaries indicating complex interaction between natural forces and human activities that have together molded coastal sediment features.

The transportation of ores and pellets by mechanized barges along the Mandovi and Zuari estuaries to Mormugao Harbour for export plays a significant role in the material input to the river and estuarine system.

At 8.78m, the grain size is fine grain, however at 12.14m, the grain size is medium grained, this could possibly indicate that there could be possibly 2 cycles of deposition, however there being no samples available from 8.78m to 12.14m, One cannot conclusively say that there are 2 cycles of deposition.

## RESULT

In the sediment core, metagreywacke, the country rock, was found at a depth of 25.4 m, belonging to Sanvordem formation followed with samples available from 8.78m, 12.14m, 14.99m, 18.06m, 21.06m and 25.4m. This sequence primarily consists of muddy sand and slightly muddy sand containing kaolinite, haematite, goethite, illite, and quartz. Hydrodynamic conditions were assessed by plotting data for each sample, indicating that samples (Figure No.14) 2 (12.14m), 3(14.99m), 4(18.06m), and 5(21.06m) belong to a turbulent environment, while sample 1(8.78m) is in a moderately turbulent environment. XRD analysis of clay fraction revealed the presence of illite, quartz, kaolinite, haematite, and goethite.

## REFERENCES

Arolkar, D. B. (1995). Petrology of the Bondla Mafic Ultramafic Complex, Usgaon, Goa, with special reference to Chromite Mineralisation (Doctoral dissertation, Goa University)

Awasthi, A. K. (1970). Skewness as an environmental indicator in the Solani river system, Roorkee (India). *Sedimentary Geology*, 4(1-2), 177-183.

Bardhan, Subhendu & Ghosh, Tuhin & Mondal, Subhronil & Roy, Arindam & Mallick, Sumanta. (2011). The Holocene sea level changes as evidenced from palaeontological data: A case study from *Glaucanome sculpta* (Bivalvia) along the eastern coast of India. *Palaeoworld*. 20. 92-97. 10.1016/j.palwor.2010.10.001.

Bhaskar, P. V., Cardozo, E., Giriyan, A., Garg, A., & Bhosle, N. B. (2000). Sedimentation of particulate matter in the Dona Paula Bay, west coast of India during November to May 1995–1997. *Estuaries*, 23, 722-734.

Bunaciu, Andrei A. & UdrişTioiu, Elena & Aboul-Enein, Hassan. (2015). X-Ray Diffraction: Instrumentation and Applications. *Critical reviews in analytical chemistry / CRC*. 45. 10.1080/10408347.2014.949616.

Ciftci, Hakan. (2021). An Introduction to Montmorillonite Purification. 10.5772/intechopen.98188.

Cochrane, S. (2014). The Munsell Color System: A scientific compromise from the world of art. *Studies in History and Philosophy of Science Part A*, 47, 26-41.

Dehadrai, P. V. (1970, August). Observations on certain environmental features at the Dona Paula point in Marmugao Bay, Goa. In *Proceedings/Indian Academy of Sciences* (Vol. 72, No. 2, pp. 56-67). New Delhi: Springer India

Dessai, A. G. (2011). The geology of Goa Group: revisited. *Journal of the Geological Society of India*, 78, 233-242.

Fernandes, G. Q. (2018). Geology and characteristics of metagreywacke and associated rocks of Goa Group, India (Doctoral dissertation, Goa University).

Fernandes, G. Q., Iyer, S. D., & Kotha, M. (2022). Styles and origin of post-and syn-depositional structures of metagreywacke-argillite strata (Goa Group), and formation of Bouma sequence, West Coast of India. *Journal of Sedimentary Environments*, 7(2), 237-250.

Flemming, B.W., 2000. Geology, morphology and sedimentology of estuaries and coasts. *Treatise of Estuarine and Coastal Science*, Volume 3/ Chapter 2.

Flemming, B.W., 2000. A revised textural classification on the basis of ternary diagrams. *Continental Shelf Research* 20, 1125-1137.

Folk, R.L. & Ward, W. 1957. Brazos River Bar: A Study in the Significance of GrainsSize Parameters. *Jour. Sed. Pet.*, 27, 3-26. Kale, V. S., 1983. Neogene and Quaternary geomorphology of the Zuari and Mandovi river basins Goa. Ph. D. Thesis, University of Pune (unpublished).

Gaonkar, C.V. & Nasnodkar, Maheshwar. (2021). Assessment of metal enrichment and contamination in surface sediment of Mandovi estuary, Goa, West coast of India. *Environmental Science and Pollution Research*. 28. 10.1007/s11356-021-14610-1.

Kale, V. S., and Rajaguru, S. N., 1985. Neogene and Quaternary transgressional and regressional history of the west coast of India- An overview. *Deccan College Bull.*, Pune. 153-163

Kumari, Neeraj & Mohan, Chandra. (2021). Basics of Clay Minerals and Their Characteristic Properties. 10.5772/intechopen.97672.

Mörner, N. A. (2017). Coastal morphology and sea-level changes in Goa, India during the last 500 years. *Journal of Coastal Research*, 33(2), 421-434.

Nair, R. R., and Hashimi, N.H., 1980. Holocene climatic influence from the sediments of the western Indian continental shelf. *Proc. Ind. Acad. Sci.*, 89: 299-315

Quinn, P. S., & Benzonelli, A. (2018). XRD and materials analysis. *The encyclopedia of archaeological sciences*, 1-5.

Reddy, G. V., & Sastry, J. S. (1988). Aeolian sand transport and its effects on the stability of Miramar-Caranzalem beach. *Mahasagar*.

Sebastian, T., Nath, B. N., Naik, S., Borole, D. V., Pierre, S., & Yazing, A. K. (2017). Offshore sediments record the history of onshore iron ore mining in Goa State, India. *Marine pollution bulletin*, 114(2), 805-815

Shetye, S.R. & Shankar, D. & S., Neetu & Suprit, K. & Michael, G Selvan & Chandramohan, P.. (2007). The environment that conditions the Mandovi and Zuari estuaries. *The Mandovi and Zuari estuaries*.

Sonak, S. M. (2017). *Marine shells of Goa*. Goa: Springer International Publishing.

Wentworth, C. K. (1922). A scale of grade and class terms for clastic sediments. *The journal of geology*, 30(5), 377-392.